Bone Marrow Niche Trafficking of miR-126 Controls Quiescence and Self-Renewal of Leukemia Stem Cells in Chronic Myelogenous Leukemia

Bin Zhang[1‡*], Le Xuan Truong Nguyen[1,2‡], Ling Li[1], Dandan Zhao[1], Bijender Kumar[1], Herman Wu[1], Allen Lin[1], Francesca Pellicano[3], Lisa Hopcroft[3], Yu-Lin Su[4], Mhairi Copland[3], Tessa L. Holyoake[3], Calvin J. Kuo[5], Ravi Bhatia[6], David S. Snyder[1], Haris Ali[1], Anthony S. Stein[1], Casey Brewer[1], Huafeng Wang[1,7], Tinisha McDonald[1], Piotr Swiderski[1], Estelle Troadec[1], Ching-Cheng Chen[1], Adrienne Dorrance[8], Vinod Pullarkat[1], Yate-Ching Yuan[1], Danilo Perrotti[9], Nadia Carlesso[1], Stephen J. Forman[1], Marcin Kortylewski[4#], Ya-Huei Kuo[1#], Guido Marcucci[1#*]

[1]Gehr Family Center for Leukemia Research, Hematology Malignancies and Stem Cell Transplantation Institute, City of Hope Medical Center, Duarte CA

[2]Department of Medical Biotechnology, Biotechnology Center of Ho Chi Minh City, Vietnam

[3] Paul O'Gorman Leukemia Research Centre, College of Medical, Veterinary & Life Sciences, Institute of Cancer Sciences, University of Glasgow, Scotland, UK

[4]Department of Immuno-Oncology; City of Hope Medical Center, Duarte CA

[5]Stanford University School of Medicine, Stanford, CA;

[6]University of Alabama at Birmingham, Birmingham, AL;

[7]Department of Hematology, the First Affiliated Hospital, Zhejiang University school of medicine, Hangzhou, Zhejiang, PR China

[8]Ohio State University; Columbus OH;

[9]University of Maryland, Baltimore, MD

[‡]These authors contributed equally

[#]These senior authors contributed equally

Running title: Eliminating CML LSC by targeting niche-mediated miR-126

Keywords: microRNA, BM niche, CML, LSC, chemoresistance

*Correspondence should be addressed to: Bin Zhang and Guido Marcucci, City of Hope Medical Center, 1500 E Duarte Road, Duarte CA 91010. Phone: 626-256-4673; FAX: 626-301-8973. Email: bzhang@coh.org or gmarcucci@coh.org

Conflict of interest: none

Abstract

Chronic myelogenous leukemia (CML) stem cells (LSC) are responsible for initiating and maintaining clonal hematopoiesis. These cells persist in the bone marrow (BM) despite effective inhibition of the BCR-ABL kinase activity by tyrosine kinase inhibitors (TKI). Here, we show that miR-126 supports quiescence, self-renewal and engraftment capacity of CML LSC. However, despite this key role, endogenous miR-126 is decreased in CML LSC compared to the normal counterpart of long-term hematopoietic stem cells (LTHSC), through a BCR-ABL-dependent mechanism involving interactions between phosphorylated-SPRED1 and RAN, inhibition of the RAN/EXP-5/RCC1 complex, and subsequent interference of mature miR-126 biogenesis. Endothelial cells (EC) in the BM then supply miR-126 to CML LSC to support quiescence and leukemia growth as we showed using genetic CML models with conditional miR-126 knock-out (KO) in EC and/or LSC. Notably, by inhibiting BCR-ABL, TKI treatment causes an undesired increase in endogenous miR-126 levels, thereby enhancing LSC quiescence and persistence. Genetic miR-126 KO in LSC and/or EC, or treatment with a novel CpG-miR-126 inhibitor targeting miR-126 in both LSC and EC enhances the *in vivo* anti-leukemic activity of TKI and significantly diminishes LSC leukemia-initiating capacity, thereby providing a novel and effective strategy to eliminate LSC in CML.

Introduction

Chronic myelogenous leukemia (CML) is a clonal myeloproliferative disorder characterized at the cytogenetic level by the translocation of chromosomes 9q34 and 22q11[1], which creates a fusion gene, *BCR-ABL* that encodes a constitutively activated tyrosine kinase responsible for transforming normal hematopoietic stem cells (HSC) into leukemia stem cells (LSC). This ultimately leads to growth factor-independent proliferation and enhanced survival of clonal HSC and hematopoietic progenitor cells (HPC), resulting in a clinically uncontrolled myeloproliferation that eventually evolves into fatal blast crisis if left untreated. CML long-term (LT) HSC (or LSC) are at the apex of malignant clonal hematopoiesis and initiate and maintain leukemia growth. In CML, LSC activity is restricted to the LTHSC-enriched $Lin^-CD34^+CD38^-CD90^+$ population for humans, and the $Lin^-Sca\text{-}1^+c\text{-}Kit^+Flt3^-CD150^+CD48^-$ population for mice[2]. CML LSC are thought to reside in a leukemia niche that may be anatomically and functionally different from that of normal HSC.

Currently, oral tyrosine kinase inhibitors (TKI) are used as the first-line treatment to induce long-term disease remission in CML patients. Although most patients treated with TKI monotherapy achieve major clinical and molecular responses, cells from the original *BCR-ABL* clone frequently persist, likely due to the failure of these agents to eliminate CML LSC[3], and treatment discontinuation frequently results in disease relapse. Thus, identification of mechanisms that support CML LSC homeostasis is clinically relevant as it may enable us to design novel targeting strategies aimed at a complete disease elimination and discontinuation of expensive life-long TKI therapy, without increased risk of disease progression.

MicroRNAs (miRNAs) are short non-coding RNAs that regulate translation of target messenger RNAs (mRNAs) into proteins that are involved in homeostatic mechanisms of normal cells[4]. Deregulation of endogenous miRNA production and abnormal extracellular trafficking have been

reported in both solid tumors and hematologic malignancies, including acute and chronic leukemia, and have been shown to play relevant roles in initiation and maintenance of malignant cellular clones[5]. In particular, miR-126-3p (miR-126) highly expressed in normal HSC and HPC restrain these cells from engaging into cell-cycle progression during hematopoiesis[6]. Our group and others have also shown that increased miR-126 expression enhances the frequency of quiescent LSC and is associated with a worse outcome in acute myeloid leukemia (AML)[7-10]. More recently, stable up-regulation of miR-126 in a mouse model led to development of acute lymphoblastic leukemia[11]. Thus, these results establish a key role for miR-126 in normal and clonal hematopoiesis.

It is also known that miR-126 is specifically and highly expressed in endothelial cells (EC) and regulates angiogenesis[12]. Anatomical and functional connections between the endothelium and normal HSC that regulates normal hematopoiesis have recently been reported[13]. Herein we hypothesized that miR-126 may also mediate a similar functional interplay between EC and LSC in the leukemia BM niche and in turn regulate CML growth. Consistent with this hypothesis, we showed that EC supply miR-126 to CML LSC to modulate quiescence and self-renewal clonal activities. In fact endogenous miR-126 in CML LSC was shown to be down-regulated through SPRED1 which was phosphorylated by BCR-ABL and interfered with Exportin-5 (Exp-5)-mediated miR-126 biogenesis. Thus, to achieve levels of mature miR-126 sufficient to sustain quiescence and preserve clonal hematopoiesis, CML LSC relied on exogenously supplied miR-126 from EC. We demonstrated the biological relevance of miR-126 trafficking from EC to CML LSC in the leukemia niche using genetic miR-126 knock-out (KO) mouse models. Notably, as BCR-ABL down-regulated miR-126, inhibition of BCR-ABL by TKI led to an undesired increase in endogenous miR-126 levels and in turn in the frequency of quiescent CML LSC with repopulating capacity. Consistent with these results, we showed that the combination of TKI

with a novel miR-126 inhibitor targeting miR-126 in both EC and CML LSC cells led to the elimination of CML LSC.

Results

Higher miR-126 levels are associated with human and mouse CML LSC

Immunophenotypically defined subsets of HPC [$Lin^-CD34^+(CD34^+)$ and $Lin^-CD34^+CD38^+$ ($CD38^+$)], HSC [$Lin^-CD34^+CD38^-$ ($CD38^-$) and $Lin^-CD34^+CD38^-CD90^-$ ($CD90^-$)] and LTHSC [$Lin^-CD34^+CD38^-CD90^+$ ($CD90^+$)] were sorted from normal donors' (n=12) and newly diagnosed chronic phase (CP) CML patients' (n=12) peripheral blood (PB) and BM samples. miR-126 expression was measured using quantitative RT-PCR (QPCR). LTHSC in both normal and CML samples showed the highest expression of miR-126 (Fig. 1a, b).

Similar results were obtained in wild-type (WT) B6 and inducible SCLtTA/BCR-ABL transgenic B6 mice, a well established CML mouse model[14]. $Lin^-Sca\text{-}1^-c\text{-}Kit^-$ ($L^-S^-K^-$), $Lin^-Sca\text{-}1^-c\text{-}Kit^+$ ($L^-S^-K^+$) [including common myeloid progenitors (CMP), granulocyte-macrophage progenitors (GMP) and megakaryocyte-erythrocyte progenitors (MEP)], $Lin^-Sca\text{-}1^+c\text{-}Kit^+$ (LSK) and LTHSC (LSK $Flt3^-CD150^+CD48^-$) cells were isolated from the BM of WT mice and CML mice after BCR-ABL induction by tetracycline withdrawal (Supplementary Fig. 1a). As in human samples, normal and CML LTHSC showed the highest expression of miR-126 (Fig. 1c, d).

The association of miR-126 with quiescence in CML LSC was proven by transducing human CML $Lin^-CD34^+CD38^-$ cells (HSC) and mouse CML LTHSC with GFP-expressing miRZip anti-miR-126 (miR-126 KD) or miR-126 precursor (overexpression, OE) lentiviral vectors. GFP^+ cells were selected and cultured for 72 hours (h) in StemSpan™ Serum-Free Expansion Medium II (SFEM II) supplemented with low concentrations of growth factors (GF)[15]. Results for human HSC are shown in Fig. 1e-i and for mouse LTHSC in Fig.1j-m. miR-126 KD increased cell cycling and apoptosis, decreased colony forming cells (CFC) and CFC replating efficiency.

Conversely, miR-126 OE decreased cell cycling and apoptosis, and increased CFC replating efficiency. We validated these results in vivo, first showing that quiescent Hoechst^{-}Pyronin^{-} (G0) fraction of CML LTHSC from the induced SCLtTA/BCR-ABL mouse (CD45.2) expressed significantly higher miR-126 levels than the proliferating Hoechst$^{+/-}$Pyronin^{+} (G1/G2/S/M) fraction of CML LTHSC (p= 0.0019; Fig. 1n), and then demonstrating that the quiescent CML LTHSC had a significantly higher rate of long-term engraftment and leukemogenic capacity than the proliferating CML LTHSC after transplant into CD45.1 congenic recipient mice (Fig. 1o-p).

BCR-ABL down-regulates miR-126 expression in CML cells

While miR-126 has similar patterns of expression and function in CML as in normal hematopoiesis[6], we noted that miR-126 levels were consistently lower in CML subpopulations compared to their normal counterparts, in both human and mouse. In human samples, CML Lin^{-}CD34^{+}CD38^{-} (HSC) and Lin^{-}CD34^{+}CD38^{-}CD90^{+} cells (LTHSC) had significantly lower miR-126 levels than their normal counterparts (Fig. 2a-b), and significant differences were also observed in the mouse (Fig. 2c). Consistent with this finding, CML HSC and LTHSC expressed higher levels of *PIK3R2* and *SPRED1*, two validated targets known to be suppressed by miR-126[6,9,12,16,17], than their normal counterparts (Supplementary Fig.1b, c).

The differential expression of miR-126 observed between normal and CML cells led us to postulate that BCR-ABL itself was involved in lowering endogenous miR-126 levels in CML cells. To test this hypothesis, normal mouse BM LSK cells were transduced with a *BCR-ABL* retroviral or control vector and GFP^{+} cells were selected and cultured for 3 days. Upon *BCR-ABL* induction (Fig. 2d), miR-126 expression decreased (Fig. 2e) and *PIK3R2* and *SPRED1* increased compared to the control cells (Supplementary Fig. 1d, e) along with a concurrent increase in cell cycling (Fig. 2f) and cell growth (Fig. 2g) rates. To further validate this finding,

LTHSC from non-induced BCR-ABL transgenic mice were sorted and cultured with or without tetracycline (2µg/ml). Upon tetracycline withdrawal and BCR-ABL induction (Fig. 2h), we observed reduced miR-126 levels (Fig. 2i) and increased cell cycling (Fig. 2j) and cell growth (Fig. 2k) rates compared with non-induced controls. Conversely, BCR-ABL inhibition using 2 or 5 µM nilotinib (NIL), a first-line TKI for CML treatment, led to increased miR-126 expression (Fig. 2l-n), decreased *PIK3R2* and *SPRED1* levels (Supplementary Fig. 1f, g) and an increased fraction of quiescent cells in the human CML HSC population (Fig. 2o), but not in normal counterpart (Supplementary Fig. 1h), compared with vehicle alone. BCR-ABL inhibition with NIL also resulted in increased miR-126 expression in human BCR-ABL$^+$ K562 cells (Supplementary Fig. 1i).

BCR-ABL deregulates miR-126 biogenesis

While CML cells harbored lower levels of mature miR-126 than normal cells, we noted that BCR-ABL-positive cells had higher levels of primary (pri-) and precursor (pre-) miR-126 (Fig. 3a, b). This led us to hypothesize that BCR-ABL could interfere with miR-126 biogenesis.

RAN (RAS-related nuclear protein) is a GTP-binding nuclear protein and a member of the RAS super family. It forms a protein complex with Exp-5 and RCC1, which are involved in miRNA nucleus-to-cytoplasm shuttling and maturation[18]. SPRED1 requires activation via tyrosine phosphorylation to act as a negative regulator of the members of the RAS superfamily[19]. We therefore postulated that the BCR-ABL tyrosine kinase may phosphorylate SPRED1, allowing SPRED1 to bind with RAN and in turn interfere with RAN/Exp-5/RCC1-mediated shuttling and maturation of miR-126 in CML cells. Using immunofluorescence (IF), immunoprecipitation (IP) and *in vitro* kinase activity assays of BCR-ABL$^+$ primary CD34$^+$ and/or K562 cells, we showed that SPRED1 co-localized with BCR-ABL to the cytoplasm (Fig. 3c), was directly phosphorylated by BCR-ABL (Fig. 3d), and formed an intra/perinuclear protein complex with

RAN whose binding with Exp-5/RCC1 complex decreased (Fig. 3e, f). NIL treatment reversed these effects, resulting in SPRED1 de-phosphorylation (Fig.3d, left panel), decreased interaction and co-localization of SPRED1 with RAN (Fig. 3f), increased RAN/Exp-5/RCC1 complex (Fig. 3g-h), decreased pri- and pre-miR-126 levels, and increased mature miR-126 levels (Fig. 3i). Cell washing to remove NIL restored the binding of SPRED1 with RAN, decreased the binding of RAN with Exp-5/RCC1 (Fig. 3j), increased levels of pri-miR-126 (Fig. 3k) and reduced levels of mature miR-126 (Fig. 3k, l). Northern blotting confirmed that the ratio of pri- and pre-miR-126 to mature miR-126 decreased upon exposure of BCR-ABL$^+$ cells to NIL and increased upon NIL washing-off (Fig. 3m). SPRED1 knock-down (KD) by siRNA in BCR-ABL$^+$ primary CD34$^+$ and K562 cells consistently enhanced formation of the RAN/Exp-5/RCC1 complex (Fig. 3n) and resulted in decreased pri- and pre-miR-126 (Fig. 3o) and increased mature miR-126 (Fig. 3o, p). Finally, RAN KD by siRNA resulted in increased pri- and pre-miR-126 and reduced mature miR-126 levels (Fig. 3q-r).

We conclude that in CML cells, miR-126 levels are reduced through BCR-ABL-induced SPRED1 phosphorylation that interferes with RAN/Exp-5/RCC1-mediated miR-126 biogenesis. Given that miR-126 suppresses SPRED1, reduced levels of mature miR-126 are likely to cause a further increase in SPRED1, thereby amplifying an autoregulatory microcircuit, through which endogenous levels of miR-126 are controlled by its own target (SPRED1) and are progressively reduced in BCR-ABL$^+$ cells via a feedback loop.

Endothelial cells in the niche supply miR-126 to CML LTHSC

Given that miR-126 is necessary for quiescence of LTHSC, and BCR-ABL activation causes down-regulation of mature miR-126 and cell cycle engagement, we then reasoned that BCR-ABL$^+$ LTHSC may be supported by an exogenous source of miR-126 to maintain quiescence

and cell cycle control and ultimately prevent clonal exhaustion. BCR-ABL$^+$ LTHSC mainly reside in the BM niche with multiple regulatory non-hematopoietic cell types. Previous studies have shown that miR-126 is one of the most abundantly expressed miRNAs in EC and is involved in angiogenesis[20,21]. Consistent with this, we found that BM EC (CD45$^-$Ter119$^-$CD31$^+$) expressed the highest levels of miR-126 compared with LTHSC and other BM microenvironmental stromal cell populations, including osteoblasts (OB; CD45$^-$Ter119$^-$CD31$^-$CD166$^+$Sca-1$^-$)[22] and mesenchymal stem cells (MSC; CD45$^-$Ter119$^-$CD31$^-$CD166$^-$Sca-1$^+$)[23] in both normal and CML mice (Fig. 4a, b).

Thus we hypothesized that EC could supply miR-126 to CML LTHSC. To prove this hypothesis, EC from the femur calcified bone and marrow of SCLtTA/BCR-ABL mice were sorted and transduced with a GFP-expressing miR-126 KD lentiviral or control vector (Fig. 4c). LTHSC from induced SCLtTA/BCR-ABL mice were co-cultured with GFP+ control or miR-126 KD EC or cultured alone (i.e., no EC) for 96h and analyzed for cell cycle and expansion. After we collected LTHSC in culture suspension, we also separately collected the EC-attached LTHSC by flushing them gently with PBS buffer. Complete cell detachment was confirmed by microscopy and staining for CD45 to exclude EC contamination. CML cells co-cultured with control EC showed higher miR-126 levels (Fig. 4c), decreased cell cycling (Fig. 4d), decreased apoptosis (Fig. 4e), decreased cell growth (Fig. 4f), and increased frequency of LTHSC (Flt3$^-$CD150$^+$CD48$^-$ LSK) (Fig. 4g), compared to the cells co-cultured with miR-126 KD EC or cultured alone. The highest miR-126 levels were found in the LTHSC attached to control EC (Fig. 4h). CML LTHSC (CD45.2, 1000 cells/mouse) co-cultured with control or miR-126 KD EC, or cultured alone, for 96h were then transplanted into congenic CD45.1 recipient mice. CML LTHSC co-cultured with control EC generated higher white blood cell (WBC) counts, higher CML engraftment levels and reduced survival (p=0.04) in recipient mice, compared with CML LTHSC co-cultured with miR-126 KD EC or cultured alone (Fig. 4i-k).

A recent report showed that in normal BM, Sca-1$^+$ EC from arterial blood vessels are associated with quiescent HSC, whereas Sca-1$^-$ EC from permeable sinusoidal blood vessels are associated with proliferative HSC[13]. We then hypothesized that a similar association between EC immunophenotypic subpopulations and adjacent LTHSC cell-cycle status may exist in CML mice and, given the role of miR-126 in cell quiescence, correlate with miR-126 levels. In fact, upon sorting EC and LTHSC from endosteal marrow (endosteal) and central marrow (central) of CML (and normal) mice, we found that >70% of endosteal EC were Sca-1$^+$ and >80% of central EC were Sca-1$^-$, Sca-1$^+$ EC expressed higher miR-126 levels than Sca-1$^-$ EC, therefore, overall endosteal EC had higher miR-126 levels than central EC (Fig. 4l-o). Accordingly, endosteal LTHSC showed higher levels of miR-126 (Fig. 4p) and were more quiescent compared to central LTHSC (Fig. 4q-s). These results demonstrate a direct association between miR-126 levels in EC and cell cycle status of adjacent LTHSC, and support an active trafficking of miR-126 from EC to LTHSC *in vivo*.

To verify the support role of EC-supplied miR-126 for leukemia growth, we generated CML or normal mice with miR-126 conditional knock-out (c-KO) in LTHSC/LSC or EC or both. We crossed miR-126(c-KO) mice (gift of Dr. Calvin Kuo) with Mx1-cre+, Tie2-cre+ and SCLtTA/BCR-ABL transgenic mice to obtain conditional miR-126 KO in the following strains: miR-126(c-KO)/Mx1-cre, SCLtTA/BCR-ABL/miR-126(c-KO)/Mx1-cre, miR-126(c-KO)heterozygous(het)/Tie2-cre and miR-126(c-KO)homozygous(hom)/Tie2-cre. After injecting miR-126(c-KO)/Mx1-cre+ (Mx1+) mice with polyinosine-polycytosine (pIpC) to obtain miR-126 KO in normal HSC, we observed no significant changes in WBC counts in PB (not shown) or BM mononuclear cell subpopulations (including LTHSC) compared to control (Mx1-) mice after 16 weeks of follow-up (Fig. 5a-b). Targeted miR-126 KO in CML LSC was then obtained with tetracycline withdrawal to induce BCR-ABL expression and pIpC injection to induce “cre”

activation in SCLtTA/BCR-ABL/miR-126(c-KO)/Mx1+ mice. Reduction of miR-126 levels by 60% (Fig. 5c) resulted in a significantly delayed CML development (p=0.047) and increased survival (p=0.04) in SCLtTA/BCR-ABL/miR-126(c-KO)/Mx1+ mice compared with SCLtTA/BCR-ABL/miR-126(c-KO)/Mx1- controls (Fig. 5d-e).

To confirm that these results were not attributable to “leaky” miR-126 down-regulation in the non-hematopoietic compartment, CD45.2 CML LTHSC from BCR-ABL-induced and pIpC-injected SCLtTA/BCR-ABL/miR-126(c-KO)/Mx1+ or Mx1- mice were sorted and transplanted into CD45.1 congenic recipient mice (Fig. 5f). Recipients transplanted with Mx1+ (miR-126 KO) CML LTHSC (Fig. 5g) showed a similar trend for decreased CML development and increased survival compared with recipient mice transplanted with Mx1- control CML LTHSC (Fig. 5h-j).

To assess the contribution of EC-derived miR-126 to leukemia growth, we then sorted LTHSC from BCR-ABL-induced CD45.1/CD45.2 SCLtTA/BCR-ABL mice (generated by crossing CD45.2 SCLtTA/BCR-ABL B6 mice with CD45.1 B6 mice to track donor cells) and transplanted them into CD45.2 congenic miR-126(c-KO)/Tie2-cre- (Tie2-) (WT miR-126 in EC), miR-126(c-KO)het/Tie2-cre+(Tie2+) (heterozygous miR-126 KO in EC), or miR-126(c-KO)hom/Tie2+ (homozygous miR-126 KO in EC) recipient mice (Fig. 5k). Both het and hom Tie2+ recipient mice showed reduced CML cell engraftment, delayed CML development and significantly increased survival compared with Tie2- recipients at 16 weeks after transplant (Fig. 5l-o; p=0.009 and 0.0003 for survival of het Tie2+ and hom Tie2+ mice respectively), with a miR-126 dosage effect (70% of hom Tie2+ mice versus 10% of het Tie2+ mice were alive at 28 weeks; Fig. 5o). Of note, CD45.1 normal LTHSC did not generate a significant difference in donor cell output in PB and BM from CD45.2 miR-126(c-KO)het/Tie2+ recipients compared with miR-126(c-KO)het/Tie2- recipients after 16 weeks of follow-up (not shown).

Next, CML LTHSC from BCR-ABL-induced and pIpC-injected SCLtTA/BCR-ABL/miR-126(c-KO)/Mx1+ or Mx1- mice were transplanted into miR-126(c-KO)het/Tie2+ or Tie2- recipient mice, respectively (Fig. 5p) to assess the functional impact of a concurrent miR-126 KO in both LTHSC and EC. Tie2+ mice transplanted with Mx1+ CML LTHSC showed a significantly delayed CML development ($p=0.007$) and prolonged survival ($p=0.002$) compared with Tie2- mice transplanted with Mx1- CML LTHSC (Fig. 5q-r). At day 200, 83% of the mice with miR-126 KO in both EC and LTHSC, but none of the controls with normal miR-126 in both EC and LTHSC, were alive.

These results support a relevant role of the EC-derived miR-126 in sustaining leukemia growth in the CML LSC niche, and provide insights into a novel microenvironment-driven miRNA regulatory mechanism of CML leukemogenesis.

To validate these results in humans, we first showed that human umbilical vein EC (HUVEC) expressed significantly higher levels of miR-126 compared with human CML $CD34^+$ subpopulations (Supplementary Fig. 2a). We performed miR-126 KD in HUVEC using lentiviral or control (ctrl) vector transduction (Supplementary Fig. 2b, c), and co-cultured CML Lin^- $CD34^+CD38^-$ cells (HSC) with miR-126 KD or ctrl HUVEC for 96h. CML HSC co-cultured with ctrl HUVEC had significantly higher miR-126 expression (Supplementary Fig. 2d, e) and decreased cell cycle entry and apoptosis (Supplementary Fig. 2f-h) compared with CML cells co-cultured with KD HUVEC or cultured alone. We detected an increased proportion of $CD34^+$ cells among CML cells co-cultured with ctrl HUVEC compared with CML cells co-cultured with KD HUVEC or cultured alone for 96h (Supplementary Fig. 2i). CML $CD34^+$ cells co-cultured alone or with ctrl or miR-126 KD HUVEC for 96h were then transplanted into irradiated (300cGy)

NSG-SGM3 (NOD-scid gamma IL3, GM-CSF, SCF triple transgenic) mice. BCR-ABL expression in BM cells collected at 16 weeks after transplantation confirmed CML cell engraftment in recipient mice (Supplementary Fig. 2j). We observed a significant increase in human $CD45^+$ cell engraftment in mice receiving cells co-cultured with ctrl HUVEC compared with the mice receiving cells co-cultured with KD HUVEC or cultured alone (Supplementary Fig. 2k-l).

To determine the mechanisms of intercellular miR-126 trafficking between EC and HSC, we first isolated EVs from ctrl and miR-126 KD HUVEC by differential ultracentrifugation method. Using electron microscopy and nanoparticle tracking analysis by NanoSight, we determined that the size range of the EVs isolated from the supernatants of both control and miR-126 KD HUVEC was 40-150 nm (peaks at 105 and 125 nm, respectively, Supplementary Fig. 3a-b). By western blot, we showed expression of exosome-specific proteins (i.e., CD63, TSG101) and EV-associated protein (i.e., HSP90)[24,25] and lack of the non EV-associated protein (i.e., the mitochondrial protein Cytochrome C) in EVs recovered from HUVEC (Supplementary Fig. 3c). Next, we isolated a fraction from HUVEC-derived EVs using magnetic beads coated with anti-CD63 antibody. We confirmed expression of exosome-specific proteins on this EV fraction using antibodies to tetraspanins (i.e., CD63, CD9 and CD81) by Cytofluorimetric analysis (Supplementary Fig. 3d). Significantly higher miR-126 levels were found in $CD63^+$ EV fraction compared with $CD63^-$ EV fraction by QPCR (0.77 versus 0.19, Supplementary Fig. 3e). These results suggest that EVs from HUVEC contain miR-126. Notably the highest miR-126 levels were detected in the EVs obtained from ctrl HUVEC compared to those obtained from miR-126 KD HUVEC or from human normal and CML $Lin^-CD34^+CD38^-$ HSC cells (Supplementary Fig. 3f).

To demonstrate the intercellular trafficking of miR-126, we labeled miR-126 with a fluorescence probe in cultured HUVEC cells (Supplementary Fig. 3g), subjected the supernatant from these cells to differential ultracentrifugation and added the collected EVs to BCR-ABL$^+$ K562 cells in culture. A miR-126 fluorescence signal was then detected in the K562 cells by confocal microscopy (Supplementary Fig. 3h). To corroborate these results, human CML HSC were cultured for 96h with EVs (5x10^9 particles/ml measured by NanoSight, equivalent to 5µg/ml measured by standard protein quantification method) isolated from ctrl or KD HUVEC or cultured alone. CML HSC co-cultured with ctrl HUVEC-derived EVs had significantly increased miR-126 levels (Supplementary Fig. 3i) and reduced cell cycling and apoptosis rates (Supplementary Fig. 3j-m) compared with the cells co-cultured with KD HUVEC-derived EVs or cultured alone. Furthermore, miR-126 KO CML LTHSC from BCR-ABL-induced and pIpC-injected SCLtTA/BCR-ABL/miR-126(c-KO)/Mx1-cre+ mice were co-cultured with ctrl or miR-126 KD HUVEC-derived EVs or cultured alone for 48 hours. MiR-126 KO CML cells co-cultured with ctrl HUVEC-derived EVs showed significantly increased miR-126 levels (Supplementary Fig. 3n) and reduced cell cycling and apoptosis rates (not shown) compared with the cells co-cultured with KD HUVEC-derived EVs or cultured alone.

Primary CML CD34$^+$ cells co-cultured with EVs (5x10^9 particles/ml) from ctrl or miR-126 KD HUVEC for 96h were then transplanted into NSG-SGM3 mice. The mice receiving cells co-cultured with ctrl HUVEC-derived EVs showed enhanced human CD45$^+$ (p=0.001; Supplementary Fig.3o) and CD45$^+$CD34$^+$ (p=0.0008; Supplementary Fig.3p) BM engraftment at 16 weeks, compared with mice receiving cells co-cultured with KD HUVEC-derived EVs. QPCR confirmed that the engrafted cells in both groups were BCR-ABL$^+$ (not shown). We also sorted CML LTHSC from induced CD45.2 SCLtTA/BCR-ABL mice and co-cultured them with ctrl or KD HUVEC-derived EVs for 96h and then transplanted into CD45.1 recipient mice. LTHSC co-

cultured with ctrl HUVEC-derived EVs showed increased miR-126 expression (p=0.009; Supplementary Fig.3q), enhanced CML progression (p=0.002), increased engraftment rate (p=0.06), and reduced survival (p=0.04) in recipient mice compared with LTHSC co-cultured with KD HUVEC-derived EVs (Supplementary Fig.3r-t). Altogether, these observations suggest that EVs-mediated trafficking carries miR-126 from EC to LTHSC.

miR-126 knockdown enhances TKI-mediated targeting of CML LSC

Given that BCR-ABL activity reduces endogenous levels of miR-126 in LTHSC and that pharmacologic inhibition of BCR-ABL by NIL increases miR-126 levels and the frequency of quiescent LTHSC (Fig. 2d-o), we then postulated that miR-126 down-regulation may enhance the anti-leukemic activity of TKI and eliminate CML LSC. To test this hypothesis, we subjected human CML HSC to miR-126 KD or OE by GFP-expressing lentiviral transduction. GFP^+ cells were selected and cultured for 4 days in SFEM II supplemented with low concentrations of GF[15], in the presence of NIL (Fig. 6a). We showed increased cell cycling and apoptosis (Fig. 6b-c) and decreased cell growth, CFC and CFC replating efficiency in the miR-126 KD and NIL-treated cells compared with NIL-treated control cells (Fig. 6d-f). Conversely, we demonstrated decreased cell cycling and apoptosis (Fig. 6b-c) and increased CFC and CFC replating efficiency in miR-126 OE and NIL-treated cells (Fig. 6e, f) compared with NIL-treated control cells. Similar results were obtained in CML LTHSC from SCLtTA/BCR-ABL mice (Fig. 6g-k).

To prove that miR-126 KD could enhance the anti-leukemic activity of TKI, human CML HSC were transduced with miR-126 KD lentiviral or control vector; selected GFP^+ cells were treated with NIL (5µM) for 4 days and then transplanted into irradiated NSG-SGM3 mice. We observed reduced engraftment of human $CD45^+$ cells in PB at 4 weeks (Fig. 6l) and in BM at 16 weeks (Fig. 6m and Supplementary Fig. 4a) in the recipient mice receiving miR-126 KD cells treated

with NIL compared to controls. QPCR analysis showed that *BCR-ABL* levels were reduced in BM cells from NSG-SGM3 mice receiving miR-126 KD CML cells (Supplementary Fig. 4b).

To test if miR-126 down-regulation in EC also enhanced the CML HSC sensitivity to TKI, we cultured human CML HSC alone or with HUVEC ± miR-126 KD, with or without NIL for 72h. We observed significantly increased apoptosis and decreased cell growth and CFC in CML HSC co-cultured with KD HUVEC compared with CML HSC cultured with ctrl HUVEC, with or without NIL (Supplementary Fig. 4c-e). Of note, CML HSC co-cultured with KD HUVEC-derived EVs also showed significantly increased apoptosis and decreased cell growth compared to CML HSC co-cultured with ctrl HUVEC-derived EVs, with or without NIL (Supplementary Fig. 4f, g). Next, CML LTHSC from induced CD45.1/CD45.2 SCLtTA/BCR-ABL mice were sorted and transplanted into CD45.2 miR-126(c-KO)het/Tie2+ or Tie2- mice. Once we confirmed CML development, we treated the mice with NIL (50mg/kg, daily by oral gavage) or vehicle for 3 weeks. Vehicle-treated Tie2+ mice showed a delayed CML development ($p=0.02$) and increased survival ($p=0.001$) compared with vehicle-treated Tie2- mice. NIL-treated Tie2+ mice showed significantly reduced WBC counts in PB ($p=0.03$) and increased survival ($p=0.02$) compared with NIL-treated Tie2- mice (Fig. 6n-p). All NIL-treated Tie2+ mice were alive at day 150. Altogether, these results support the hypothesis that miR-126 down-regulation in EC and CML HSC enhances the anti-leukemic activity of TKI.

Although the mechanistic basis for how miR-126 KD enhanced TKI activity may be related to altered expression levels of multiple miR-126 targets involved in pathways of proliferation and survival, we observed that, consistent with previous reports[26,27], NIL treatment in CML $CD34^+$ cells enhanced MAPK/ERK signaling which has been shown to promote cell survival and inhibit apoptosis through BCL-2 up-regulation (Supplementary Fig. 4h). Thus, we reasoned that NIL-induced up-regulation of miR-126 and in turn down-regulation of SPRED1 (Supplementary Fig.

4h, i), a reported inhibitor of the MAPK/ERK pathway, could contribute to this effect. In fact, miR-126 KD induced SPRED1 up-regulation and decrease of phospho-ERK (p-ERK) and BCL-2 levels (Supplementary Fig. 4j-k). Consistently, SPRED1 KD by siRNA increased p-ERK and BCL-2 levels, and rescued NIL-induced apoptosis (Supplementary Fig. 4l-o) in CML $CD34^+$ cells. NIL-induced apoptosis was enhanced by the MEK inhibitor PD0325901 or BCL-2 KD (Supplementary Fig. 4p-s). Thus, these results support a model in which NIL induces miR-126 up-regulation, decreases SPRED1, results in spurious activation of the MAPK/ERK pathway, and ultimately increases BCL-2 levels; while miR-126 KD counteracts these effects, thereby increasing the anti-leukemic activity of NIL.

Effective *in vitro* and *in vivo* uptake and gene silencing effects of the CpG-miR-126 inhibitor

Given that miR-126 KD enhanced the anti-leukemic activity of NIL, we reasoned that miR-126 is likely an effective therapeutic target to eliminate LSC. microRNAs are generally targeted with oligonucleotide therapeutics (ONTs). It remains challenging to achieve an efficient and cell-selective delivery of ONTs *in vivo*. Thus, we designed a novel miR-126 inhibitor by linking an anti-miR-126 oligodeoxynucleotide (ODN) to a cytosine guanine dinucleotide (CpG) ODN, a ligand for the intracellular Toll-like Receptor 9 (TLR9). To allow for systemic administration, the CpG-miR-126 inhibitor was chemically modified to resist serum nucleases using phosphothioation and 2'OMe-modified nucleotides in the CpG ODN and anti-miR-126 moieties, respectively. We then compared the specificity and efficiency of this novel CpG-miR-126 inhibitor uptake with a nanoparticle (NP) delivery method previously reported by our group[8]. We incubated K562 cells with fluorescently-labeled CpG-miR-126 inhibitor-Cy3 (CpG), human CD45 antibody (Ab)- or Transferrin (TF)-conjugated NPs containing miR-126 inhibitor-Cy3 (Ab-NP or TF-NP), or naked miR-126 inhibitor-Cy3 (control), in the absence of any reagent(s) routinely

used for nucleic acid transfection. Flow cytometric analysis at 4h and 24h (Supplementary Fig. 5a-b) showed that CpG-miR-126 inhibitor-Cy3 was efficiently taken up by 99% of the K562 cells at both 4h and 24h, compared with only a fraction of the cells incubated with Ab-NP (24% for 4h and 30% for 24h) or TF-NP (74% for 4h and 88% for 24h). K562 cells did not take up naked miR-126 inhibitor (control) (Supplementary Fig. 5b). Efficient miR-126 down-regulation by CpG-miR-126 inhibitor-Cy3 in K562 cells was confirmed by QPCR at 24h (Supplementary Fig. 5c). We further showed by flow cytometry that, even without routinely used transfection reagents for nucleic acids, the CpG-miR-126 inhibitor-Cy3 was internalized by HUVEC as well as human normal and CML $Lin^{-}CD34^{+}CD38^{-}$ cells at 4h (Supplementary Fig. 5d-f); >95% cells were positive for CpG-miR-126 inhibitor-Cy3 uptake in all three cell types. The efficient miR-126 down-regulation in HUVEC and HSC was also confirmed by QPCR (Supplementary Fig. 5g-i). We also observed increased cell cycling in both CpG-miR-126 inhibitor-treated normal and CML HSC compared to CpG-scrambled RNA (scrRNA)-treated controls (Supplementary Fig. 5j-k).

Next, we evaluated CpG-miR-126 inhibitor-Cy3 uptake in murine CML BM, LTHSC and EC cells *in vitro* and *in vivo*. Following *in vitro* exposure to CpG-miR-126 inhibitor-Cy3, efficient uptake at 4h and miR-126 down-regulation at 24h were confirmed by flow cytometry and QPCR, respectively (Supplementary Fig. 5l-m). We also observed increased cell cycling in normal and CML BM LTHSC treated with the CpG-miR-126 inhibitor (Supplementary Fig. 5n). Normal and CML mice were treated with one dose (5mg/kg, iv injection) of CpG-miR-126 inhibitor-Cy3. At 16h post-treatment, efficient *in vivo* uptake was demonstrated by flow cytometry, in both LTHSC (56±5%) and EC (62±3%) isolated from femurs (Supplementary Fig. 5o). After CpG-miR-126 inhibitor treatment (5mg/kg/day, iv, daily) for 3 days, LTHSC and EC were sorted and significant miR-126 down-regulation was confirmed by QPCR (Supplementary Fig. 5p-q).

CpG-miR-126 inhibitor enhances *in vivo* targeting of CML LSC in combination with TKI

Given that CpG-miR-126 inhibitor was efficiently taken up by both normal LTHSC and EC and effectively down-regulated miR-126 expression, we then tested the effect of the inhibitor in normal mice to ensure that the compound did not have hematologic toxicity. WT B6 mice were treated with CpG-scrRNA (scrRNA) or CpG-miR-126 inhibitor (inhibitor, 5mg/kg/day i.v.) for 3 weeks and BM cells were collected, analyzed and transplanted into recipient mice ($3x10^5$ BM cells/mouse). Compared with scrRNA-treated control mice, inhibitor-treated mice showed increased numbers of red blood cells (RBC), but no significant difference in WBC or platelets (PLT) in PB (Supplementary Fig. 6a-c), or in mononuclear cells, LTHSC, or EC in the BM (Supplementary Fig. 6d-f). This finding was in line with the observation that miR-126 down-regulation in normal HSC increases hematological output[6]. In the recipient mice receiving BM cells from donor mice treated with scrRNA or inhibitor, we observed no significant differences in donor cell engraftment in PB, BM or spleen (Supplementary Fig. 6g-h) or in donor LTHSC number in BM (Supplementary Fig. 6i) at 16 weeks after transplantation. These data demonstrate a lack of pre-clinical toxicity of the inhibitor for normal hematopoiesis.

We then tested the effects of the inhibitor alone and in combination with NIL on human and murine CML LTHSC *in vivo*. First we transplanted human $CD34^+$ cells from CP CML patients into NSG-SGM3 mice. At 6 weeks after transplantation, the mice were divided into 4 groups and treated with scrRNA (5mg/kg i.v. 4 times a week), inhibitor (5mg/kg, i.v. 4 times a week), scrRNA + NIL (50mg/kg, daily by oral gavage), or inhibitor + NIL for 3 weeks, followed by assessment of human cell engraftment in PB, BM and spleen. Significantly reduced human $CD45^+$, $CD45^+CD34^+CD38^-$ HSC and $CD45^+CD34^+CD38^-CD90^+$ LTHSC engraftment was seen in the BM of inhibitor+NIL treated recipient mice compared with scrRNA, inhibitor alone or NIL alone treated mice (Fig. 7a-c, Supplementary Fig. 6j). Fluorescence in situ hybridization (FISH)

analysis and QPCR confirmed that the engrafted human CD45$^+$ cells were *BCR-ABL* positive (Supplementary Fig. 6k).

Next, BM cells from SCLtTA/BCR-ABL mice (CD45.2) were transplanted into congenic B6 mice (CD45.1). Following confirmation of CML development at 4 weeks after transplantation, mice were treated as above with scrRNA, inhibitor, scrRNA + NIL, or inhibitor + NIL for 3 weeks. As EC-derived miR-126 plays a key role in LSC maintenance, we sorted BM EC from treated mice and confirmed significant miR-126 KD in total EC, Sca-1$^+$ EC and Sca-1$^-$ EC from inhibitor-treated mice compared with scrRNA-treated mice (Supplementary Fig. 6l-m). Mice receiving the combination of inhibitor + NIL had a significant reduction in the percentage of CD45.2$^+$ CML cells in PB, spleen and BM (Fig. 7d-f), and **a** significant reduction in the numbers of CML LSK and LTHSC in spleen and BM compared with all other control groups (Fig. 7g-j). A cohort of mice was followed for survival studies after 3 weeks of treatment. All of the mice treated with scrRNA alone died of leukemia within 60 days after discontinuing treatment, whereas 50% of the mice treated with inhibitor or NIL alone and 90% of the mice treated with the combination of inhibitor and NIL survived ($p=0.0012$; Fig. 7k).

To quantify the frequency of leukemia-initiating cells (LIC) after treatment, BM cells from leukemic mice treated with scrRNA, inhibitor, scrRNA + NIL, or inhibitor + NIL for 3 weeks were transplanted in limiting dilution into secondary congenic CD45.1 recipient mice. Treatment with the combination of inhibitor and NIL resulted in a significantly higher levels of depletion of LIC based on leukemia development in secondary recipient mice after 16 weeks of follow-up, compared with treatments with scrRNA alone, inhibitor alone or scrRNA + NIL (Fig. 7l). None of the secondary recipients that received BM cells from the mice treated with combination of inhibitor and NIL developed leukemia.

These results indicate that the combination of CpG-miR-126 inhibitor and NIL remarkably enhances eradication of CML LSC capable of engraftment in secondary recipients compared with NIL alone.

Discussion

We report here that a gradient of miR-126 expression follows a hierarchical order of hematopoietic differentiation, both in human and murine CML hematopoiesis, with more primitive stem cells or progenitors expressing higher levels of miR-126. Quiescent CML LTHSC have higher levels of miR-126 and a higher leukemia engraftment capacity than proliferating CML LTHSC. This finding was in line with the observation reported in normal hematopoiesis[6].

Unexpectedly, however, we observed that CML LTHSC had miR-126 levels significantly lower than their normal counterparts. This finding was consistent with a lower frequency of long-term repopulating cells observed within CML LTHSC compared to normal LTHSC, as shown by serial dilution LTHSC transplantation[2]. Indeed, we demonstrated that BCR-ABL expression lowered the levels of mature miR-126 and increased the levels of pri- and pre-miR-126, whereas pharmacologic BCR-ABL inhibition by TKI increased the levels of mature miR-126 and decreased the levels of pri- and pre-miR-126. Altogether, these data support a role of BCR-ABL in altering the biogenesis of endogenous miR-126. Of note, BCR-ABL-dependent deregulation of microRNAs is however unlikely to be restricted to down-regulation of miR-126. In fact, comparing LSK cells from non-induced versus induced CML mice, we found 33 miRNAs (including miR-126-3p and miR-126-5p, miR-125a-5p, 125b-5p, 181a-3p, 181b-5p, and 29b-3p) significantly decreased, and 75 miRNAs (including miR-142-3p and miR-142-5p, 146b-3p, 146b-5p, and 486-5p) significantly increased (Supplementary Fig. 1j), suggesting distinct BCR-ABL-dependent mechanisms of microRNA regulation.

To our knowledge, BCR-ABL-dependent down-regulation of miR-126 in CML cells and its mechanistic basis has not been previously reported. SPRED1, a validated miR-126 target[6,9,12,16,17], is a tyrosine kinase substrate known to inhibit GF-mediated activation of RAS protein family members and in turn the RAS/MAPK/ERK pathway[18]. Tyrosine residue phosphorylation is required for SPRED1 inhibition of RAS/MAPK/ERK activation[19]. We show here that SPRED1 is a substrate for BCR-ABL and that BCR-ABL/SPRED1 interplay is critical for miR-126 biogenesis. In fact, BCR-ABL-phosphorylated SPRED1 binds with RAN, a RAS family member, disrupts the RAN/Exp-5/RCC1 complex, which is involved in pre-miRNA nucleus-to-cytoplasm shuttling, and increases nuclear levels of pri- and pre-miR-126 and decreases cytoplasmic levels of mature miR-126. Conversely, BCR-ABL inhibition results in disruption of the binding of SPRED1 with RAN, and in turn enhances formation of the RAN/Exp-5/RCC1 complex, increases levels of mature miR-126 and decreases levels of pri- and pre-miR-126. Thus, we conclude that BCR-ABL mediates miR-126 down-regulation through SPRED1, which, once phosphorylated, inhibits the maturation of its miRNA regulator and in turn increases its own expression. This process likely creates an autoregulatory loop, where the higher the SPRED1 levels, the lower the mature miR-126 levels (Supplementary Fig. 1k).

However, miR-126 is necessary for normal and clonal HSC quiescence, and a continuous down-regulation of miR-126 could cause clonal exhaustion[6,10]. Therefore, we reasoned that the endogenous, aberrantly BCR-ABL-activated SPRED1/miR-126 autoregulatory loop must be interrupted in order to maintain a reservoir of quiescent CML LSC. Previous reports suggest that BM EC participate in the regulation of normal hematopoiesis[13,28]. Here, we show that among the distinct BM leukemia niche cell populations, EC express the highest levels of miR-126 and supply miR-126 to CML cells, likely through EVs trafficking. Furthermore, consistent with the previous reports showing that Sca-1$^+$ EC are associated with quiescent normal HSC and Sca-1$^-$

EC associated with proliferating normal HSC in the marrow[13], we show here that endosteal Sca-1$^+$ EC express higher levels of miR-126 and are associated with a larger quiescent fraction of BCR-ABL$^+$ LTHSC, which also express higher miR-126 levels. In contrast, central Sca-1$^-$ EC express lower levels of miR-126 and are associated with a larger proliferating fraction of BCR-ABL$^+$ LTHSC, which also express lower miR-126 levels. Our data therefore support a functional interplay between EC and HSC in CML, resulting in a non-random BM distribution of the quiescent CML LSC fraction that are more likely to be found proximal to the higher miR-126-expressing EC of the bone endosteum.

To demonstrate the functional relevance of the LTHSC-EC miR-126 interplay to leukemia growth, we created a series of genetic murine models with miR-126 KO in either LTHSC (normal or BCR-ABL$^+$) or EC or both. The decreased engraftment of CML LSC and improved survival observed in recipient mice with miR-126 KO in the endothelial compartment indicated that CML LTHSC and the BM microenvironment are functionally integrated through the miR-126 LTHSC-EC intercellular trafficking. Of note, we could not completely exclude the possibility that decreased CML LTHSC quiescence and engraftment capacity resulted from EC functional changes induced by miR-126 KD, rather than from a simple decrease of miR-126 trafficking from EC to LTHSC. However, Kuo et al. previously showed that miR-126 KO mice had no significant changes of BM EC structure[12]. Moreover, we have not observed significant changes in the morphology, growth rate or growth patterns of miR-126 KD HUVEC or mouse EC compared with controls (not shown).

Our results are clinically relevant to CML patients treated with TKI therapy. Persistence of CML LSC during TKI treatment is an active area of investigation, as these agents are remarkably potent against cycling cells, but fail to eliminate quiescent CML LSC[3]. Using primary CML cells

and CML murine models, we first showed that CML LSC resistance to TKI was likely mediated by SPRED1 de-phosphorylation caused by BCR-ABL inhibition that led to increased endogenous miR-126, which pushes LSC into a relatively treatment-refractory quiescent state. Furthermore, miR-126 up-regulation in TKI-treated CML $CD34^+$ cells resulted in decreased SPRED1, a MAPK/ERK pathway inhibitor, which in turn resulted in a spurious activation of MAPK/ERK pathway and increased cell survival, likely mediated by BCL-2[26,27]. These findings led us to hypothesize and prove, both *in vitro* and *in vivo,* that miR-126 KD in CML cells and/or EC enhances the anti-leukemic activity of TKI by counteracting the undesired miR-126 up-regulation and SPRED1 down-regulation induced by TKI. In fact, we showed 100% survival of genetically engineered CML mice with miR-126 KD EC treated with TKI, thereby proving miR-126 to be a suitable therapeutic target in CML.

Thus to apply our work to clinical translation, we designed a novel CpG-miR-126 ODN inhibitor that could be efficiently taken-up by both hematopoietic and non-hematopoietic cells in the BM niche. We have previously shown that the uptake of CpG–ODN conjugated molecules depends on endocytosis by scavenger family dextran sulfate-sensitive receptors (SRs)[29,30], which are expressed on the surface of normal and malignant myeloid cells[31,32]. Following SR-mediated internalization, CpG-conjugates bind to endosomal TLR9 and trigger their cytoplasmic release[29]. As a result, the TLR9-targeted delivery of ODNs overcomes endosomal retention, which has been identified to be the major issue hindering many delivery strategies (e.g. antibody-mediated delivery). SRs and TLR9 are both expressed on hematopoietic cells and EC[33-36], and likely facilitate the efficient intracellular delivery of CpG-miR-126 inhibitor and its prompt release for pharmacologic activity. Our results indeed showed that the CpG-miR-126 inhibitor was taken up by both LTHSC and EC with ~80% efficiency *in vitro* and 40-70% *in vivo* (depending on the cell type) and led to a significant miR-126 down-regulation that translated into reduced LTHSC quiescence and frequency. The combination of CpG-miR-126 inhibitor and TKI significantly

increased survival, compared with either agent alone or vehicle. Furthermore, no leukemia development in secondary transplanted recipients was observed, thereby supporting our initial hypothesis that CML LSC elimination can be achieved by optimal therapeutic targeting of miR-126. Importantly, we observed no hematologic toxicity in normal mice treated with CpG-miR-126 inhibitor. Secondary transplantation of BM cells from normal mice treated with scrRNA or CpG-miR-126 inhibitor did not show a significant difference in engraftment between the two groups. The enhanced *in vivo* effect of CpG-miR-126 inhibitor on TKI activity was also confirmed in a model of human CML $CD34^+$ cells engrafted in immunodeficient mice.

In summary, we report for the first time a complex interplay between BCR-ABL/SPRED1/RAN/Exp-5/RCC1 in CML LSC, resulting in down-regulation of endogenous miR-126 in CML LSC. CML LSC then rely on a microenvironment-driven trafficking of miR-126 from EC to LSC in the BM niche, to maintain a quiescent fraction of LSC with high leukemogenic capacity. Consistent with this model, we show that TKI treatment inhibits BCR-ABL-induced SPRED1 phosphorylation, which leads to an undesired increase of miR-126, down-regulation of SPRED1 and spurious activation of the MAPK/ERK pathway and increase of BCL-2. We proved that miR-126 KO enhances TKI activity *in vivo* and that this mechanism is therefore therapeutically targetable. Importantly, our novel CpG-miR-126 inhibitor, which is now being translated to the clinic, was active in both EC and LSC, and significantly enhanced the anti-leukemic activity of TKI, thereby providing a proof-of-concept that this therapeutic approach is feasible for LSC elimination in CML patients (Supplementary Fig. 6n).

Experimental procedures

Human samples

Normal PB and BM samples were obtained from donors at City of Hope National Medical Center (COHNMC). CP CML samples were obtained from patients who have not received prior TKI treatment from COHNMC and Glasgow Experimental Cancer Medicine Centre and UK SPIRIT trials. All CML samples used in this study are P210 BCR-ABL positive confirmed by FISH analysis and QPCR. Mononuclear cells were isolated using Ficol separation. $CD34^+$ cells were then isolated using a positive magnetic bead selection protocol (Miltenyi Biotech, Germany). All patients and healthy donors signed an informed consent form. Sample acquisition was approved by the Institutional Review Boards at the COHNMC and Greater Glasgow and Clyde NHS Trust, in accordance with an assurance filed with and approved by the Department of Health and Human Services, and met all requirements of the Declaration of Helsinki.

Animal studies

Inducible transgenic SCLtTA/BCR-ABL mice in the FVB/N background[14] were backcrossed to the B6 background (CD45.2) for 10 generations. Transgenic BCR-ABL mice were maintained on tetracycline water at 0.5 g/L. Withdrawal of tetracycline results in expression of BCR-ABL and generation of a CML-like disease in these mice. Unless otherwise indicated, BCR-ABL expression was induced for 2-3 weeks by tetracycline withdrawal and then BM cells (both tibias and femurs) were collected for experiments. SCLtTA/BCR-ABL mice (CD45.2, B6) were also bred with CD45.1 B6 mice to produce CD45.1/CD45.2 SCLtTA/BCR-ABL mice as donors. miR-126(c-KO) mice (B6, from Dr. Kuo, Stanford) were crossed with Mx1-cre, Tie2-cre (both from The Jackson Laboratory) and SCLtTA/BCR-ABL mice (all B6) to obtain the following strains: miR-126(c-KO)/Mx1-cre, miR-126(c-KO)/Mx1-cre/SCLtTA/BCR-ABL and miR-126(c-KO)/Tie2-

cre. Recipient mice in the CD45.1 B6 background (Charles River) were used to allow tracking of donor CD45.2 cells after transplant. Recipient mice were 6 to 8 weeks old and were irradiated at 900 cGy within 24h before transplantation. The number of mice for each study group was chosen based on the expected endpoint variation (i.e., engraftment rate and latency period of leukemia) and mice availability from distinct strains. The mice of the same gender and age were randomly divided into groups. Investigators were blinded to mice genotypes while performing treatment or monitoring engraftment or survival. Mouse care and experimental procedures were performed in accordance with federal guidelines and protocols approved by the Institutional Animal Care and Use Committee at the City of Hope.

Engraftment of human cells in immunodeficient mice

GFP^+ cells (2×10^5 cells/mouse) selected from CML $Lin^-CD34^+CD38^-$ cells transduced with miRZip anti-miR-126 (126 KD) or control lentivirus (ctrl) were cultured with or without NIL (5μM) for 96h. Cells were then harvested, washed and transplanted via tail vein injection into sublethally irradiated (300cGy) 8 week old NOD.Cg-*Prkdc*^{scid} *Il2rg*^{tm1Wjl} Tg(CMV-IL3,CSF2,KITLG)1Eav/MloySzJ mice (NSG-SGM3, The Jackson Laboratory). Engraftment of human $CD45^+$ cells in PB was monitored at 6 weeks. Mice were euthanized after 16 weeks and marrow contents of femurs, spleen cells and blood cells were obtained at necropsy. To assess human cell engraftment, cells were labeled with anti-mouse CD45 and anti-human CD45 and CD33 antibody and analyzed by flow cytometry. To assess engraftment of malignant BCR-ABL expressing cells, BM cells obtained were evaluated for *BCR-ABL* mRNA levels by QPCR[37].

***In vivo* treatment of normal and transgenic BCR-ABL mice**

BM cells (CD45.2) were obtained from SCLtTA/BCR-ABL mice at 4 weeks after induction of BCR-ABL expression by tetracycline withdrawal and transplanted by tail vein injection (10^6 cells/mouse) into recipient mice (CD45.1) irradiated at 900cGy. Blood samples were obtained 4 weeks after transplantation to confirm development of neutrophilic leukocytosis. Mice were treated with scrRNA (5mg/kg, 4 times a week by vein injection), CpG-miR-126 inhibitor (inhibitor, 5mg/kg, 4 times a week by vein injection), scrRNA + NIL (50mg/kg, daily by oral gavage), or inhibitor + NIL for 21 days. After 3 weeks of treatment, mice were euthanized and BM cells from right femur and spleen cells were analyzed for CML cell output. BM cells from the left femur of the treated mice were pooled and 4×10^6, 2×10^6, 1×10^6 and 5×10^5 cells/mouse (6 mice/dose x 4 doses x 4 conditions=96 mice) were transplanted into recipient mice (CD45.1) irradiated at 900cGy. WBC counts and CML cell engraftment was monitored every 4 weeks. The mice were euthanized at 16 weeks, followed by assessment of donor CML cell engraftment in PB, BM and spleen. The fraction of mice showing evidence of CML development at 16 weeks after secondary transplantation was determined and the frequency of LIC was calculated using Poisson statistics. Another cohort of mice was followed for survival up to 60 days after discontinuation of treatment. To determine the *in vivo* effect of the CpG-miR-126 inhibitor on normal hematopoiesis, normal mice were treated with scrRNA or inhibitor for 3 weeks, followed by assessment of WBC, RBC, PLT in PB and BM subpopulations in BM.

Statistics

Results are expressed as mean ± SEM. Comparison between groups was performed by Student's *t*-test, Wilcox rank sum test, non-parametric Mann Whitney test or ANOVA, adjusting for multiple comparisons as appropriate. The log-rank test was used to assess significant differences between survival curves. All statistical analyses were performed using Prism version 6.0 software (GraphPad Software). Sample sizes chosen are indicated in the individual figure

legends and were not based on formal power calculations to detect prespecified effect sizes. P values $\leq$0.05 were considered significant. Results shown represent mean ± SEM. $^{*}p \leq 0.05$, $^{**}p < 0.01$, $^{***}p < 0.001$.

Author contributions

BZ and LN designed and conducted experiments, analyzed data and wrote the manuscript; LL, DDZ, BK, HW, FP, YLS, CB, HW, TM and ET conducted experiments; AL, DS, HA and AS provided samples and reviewed the patients' data; PS and MK designed the CpG-miR-126 inhibitor, reviewed data and the manuscript; LH, YCY, CCC, AD, VP, NC, and DP analyzed data; CK provided the miR-126(c-KO) mouse model; RB provided the B6 SCLtTA/BCR-ABL CML mouse model; MC, TLH and SJF provided patient samples, designed experiments and reviewed the manuscript; MK and YHK designed experiments, analyzed data and reviewed manuscript; GM designed experiments, analyzed data, wrote manuscript and provided administrative support.

Acknowledgments

This work was supported in part by National Cancer Institute grants: CA205247, CA102031, CA201184, CA213131, CA180861, CA158350, CA184411; the Gehr Family Foundation and George Hoag Family Foundation; Cancer Research UK programme grant 11074/A11008; and The Howat Foundation. We acknowledge the support of the Animal Resources Center, Analytical Cytometry, Pathology (Liquid Tumor), Bioinformatics, Electron Microscopy, Light Microscopy, Integrative Genomics and DNA/RNA Cores at City of Hope Comprehensive Cancer Center supported by the National Cancer Institute of the National Institutes of Health under award number P30CA33572. We are grateful to COH Comprehensive Cancer Center, Glasgow Experimental Cancer Medicine Centre and SPIRIT trials, together with the patients and their

physicians for providing primary patient material for this study.

References

1. Sawyers, C.L. Chronic myeloid leukemia. *The New England journal of medicine* **340**, 1330-1340 (1999).
2. Zhang, B.*, et al.* Altered microenvironmental regulation of leukemic and normal stem cells in chronic myelogenous leukemia. *Cancer cell* **21**, 577-592 (2012).
3. Chu, S.*, et al.* Persistence of leukemia stem cells in chronic myelogenous leukemia patients in prolonged remission with imatinib treatment. *Blood* **118**, 5565-5572 (2011).
4. Garzon, R., Marcucci, G. & Croce, C.M. Targeting microRNAs in cancer: rationale, strategies and challenges. *Nature reviews. Drug discovery* **9**, 775-789 (2010).
5. Song, S.J. & Pandolfi, P.P. MicroRNAs in the pathogenesis of myelodysplastic syndromes and myeloid leukaemia. *Current opinion in hematology* **21**, 276-282 (2014).
6. Lechman, E.R.*, et al.* Attenuation of miR-126 activity expands HSC in vivo without exhaustion. *Cell stem cell* **11**, 799-811 (2012).
7. de Leeuw, D.C.*, et al.* Attenuation of microRNA-126 expression that drives CD34+38- stem/progenitor cells in acute myeloid leukemia leads to tumor eradication. *Cancer research* **74**, 2094-2105 (2014).
8. Dorrance, A.M.*, et al.* Targeting leukemia stem cells in vivo with antagomiR-126 nanoparticles in acute myeloid leukemia. *Leukemia* **29**, 2143-2153 (2015).
9. Li, Z.*, et al.* Overexpression and knockout of miR-126 both promote leukemogenesis. *Blood* **126**, 2005-2015 (2015).
10. Lechman, E.R.*, et al.* miR-126 Regulates Distinct Self-Renewal Outcomes in Normal and Malignant Hematopoietic Stem Cells. *Cancer cell* **29**, 602-606 (2016).
11. Nucera, S.*, et al.* miRNA-126 Orchestrates an Oncogenic Program in B Cell Precursor Acute Lymphoblastic Leukemia. *Cancer cell* **29**, 905-921 (2016).
12. Kuhnert, F.*, et al.* Attribution of vascular phenotypes of the murine Egfl7 locus to the microRNA miR-126. *Development* **135**, 3989-3993 (2008).
13. Itkin, T.*, et al.* Distinct bone marrow blood vessels differentially regulate haematopoiesis. *Nature* **532**, 323-328 (2016).
14. Koschmieder, S.*, et al.* Inducible chronic phase of myeloid leukemia with expansion of hematopoietic stem cells in a transgenic model of BCR-ABL leukemogenesis. *Blood* **105**, 324-334 (2005).
15. Bhatia, R., McGlave, P.B., Dewald, G.W., Blazar, B.R. & Verfaillie, C.M. Abnormal function of the bone marrow microenvironment in chronic myelogenous leukemia: role of malignant stromal macrophages. *Blood* **85**, 3636-3645 (1995).
16. Fish, J.E.*, et al.* miR-126 regulates angiogenic signaling and vascular integrity. *Developmental cell* **15**, 272-284 (2008).
17. Wang, S.*, et al.* The endothelial-specific microRNA miR-126 governs vascular integrity and angiogenesis. *Developmental cell* **15**, 261-271 (2008).
18. Bohnsack, M.T., Czaplinski, K. & Gorlich, D. Exportin 5 is a RanGTP-dependent dsRNA-binding protein that mediates nuclear export of pre-miRNAs. *Rna* **10**, 185-191 (2004).
19. Quintanar-Audelo, M., Yusoff, P., Sinniah, S., Chandramouli, S. & Guy, G.R. Sprouty-related Ena/vasodilator-stimulated phosphoprotein homology 1-domain-containing protein (SPRED1), a tyrosine-protein phosphatase non-receptor type 11 (SHP2) substrate in the Ras/extracellular

signal-regulated kinase (ERK) pathway. *The Journal of biological chemistry* **286**, 23102-23112 (2011).
20. Kuehbacher, A., Urbich, C., Zeiher, A.M. & Dimmeler, S. Role of Dicer and Drosha for endothelial microRNA expression and angiogenesis. *Circulation research* **101**, 59-68 (2007).
21. Welten, S.M., Goossens, E.A., Quax, P.H. & Nossent, A.Y. The multifactorial nature of microRNAs in vascular remodelling. *Cardiovascular research* **110**, 6-22 (2016).
22. Chitteti, B.R.*, et al.* CD166 regulates human and murine hematopoietic stem cells and the hematopoietic niche. *Blood* **124**, 519-529 (2014).
23. Houlihan, D.D.*, et al.* Isolation of mouse mesenchymal stem cells on the basis of expression of Sca-1 and PDGFR-alpha. *Nature protocols* **7**, 2103-2111 (2012).
24. Van Deun, J.*, et al.* The impact of disparate isolation methods for extracellular vesicles on downstream RNA profiling. *Journal of extracellular vesicles* **3**(2014).
25. Witwer, K.W.*, et al.* Standardization of sample collection, isolation and analysis methods in extracellular vesicle research. *Journal of extracellular vesicles* **2**(2013).
26. Boucher, M.J.*, et al.* MEK/ERK signaling pathway regulates the expression of Bcl-2, Bcl-X(L), and Mcl-1 and promotes survival of human pancreatic cancer cells. *Journal of cellular biochemistry* **79**, 355-369 (2000).
27. Galante, J.M., Mortenson, M.M., Bowles, T.L., Virudachalam, S. & Bold, R.J. ERK/BCL-2 pathway in the resistance of pancreatic cancer to anoikis. *The Journal of surgical research* **152**, 18-25 (2009).
28. Kunisaki, Y.*, et al.* Arteriolar niches maintain haematopoietic stem cell quiescence. *Nature* **502**, 637-643 (2013).
29. Nechaev, S.*, et al.* Intracellular processing of immunostimulatory CpG-siRNA: Toll-like receptor 9 facilitates siRNA dicing and endosomal escape. *Journal of controlled release : official journal of the Controlled Release Society* **170**, 307-315 (2013).
30. Zhang, Q.*, et al.* Serum-resistant CpG-STAT3 decoy for targeting survival and immune checkpoint signaling in acute myeloid leukemia. *Blood* **127**, 1687-1700 (2016).
31. Ewald, S.E.*, et al.* The ectodomain of Toll-like receptor 9 is cleaved to generate a functional receptor. *Nature* **456**, 658-662 (2008).
32. Nakamura, N.*, et al.* Endosomes are specialized platforms for bacterial sensing and NOD2 signalling. *Nature* **509**, 240-244 (2014).
33. Martin-Armas, M.*, et al.* Toll-like receptor 9 (TLR9) is present in murine liver sinusoidal endothelial cells (LSECs) and mediates the effect of CpG-oligonucleotides. *Journal of hepatology* **44**, 939-946 (2006).
34. Tamura, Y.*, et al.* Scavenger receptor expressed by endothelial cells I (SREC-I) mediates the uptake of acetylated low density lipoproteins by macrophages stimulated with lipopolysaccharide. *The Journal of biological chemistry* **279**, 30938-30944 (2004).
35. Yeh, Y.C., Hwang, G.Y., Liu, I.P. & Yang, V.C. Identification and expression of scavenger receptor SR-BI in endothelial cells and smooth muscle cells of rat aorta in vitro and in vivo. *Atherosclerosis* **161**, 95-103 (2002).
36. Iwasaki, A. & Medzhitov, R. Toll-like receptor control of the adaptive immune responses. *Nature immunology* **5**, 987-995 (2004).
37. Branford, S., Hughes, T.P. & Rudzki, Z. Monitoring chronic myeloid leukaemia therapy by real-time quantitative PCR in blood is a reliable alternative to bone marrow cytogenetics. *British journal of haematology* **107**, 587-599 (1999).

Figures and Legends

Figure 1

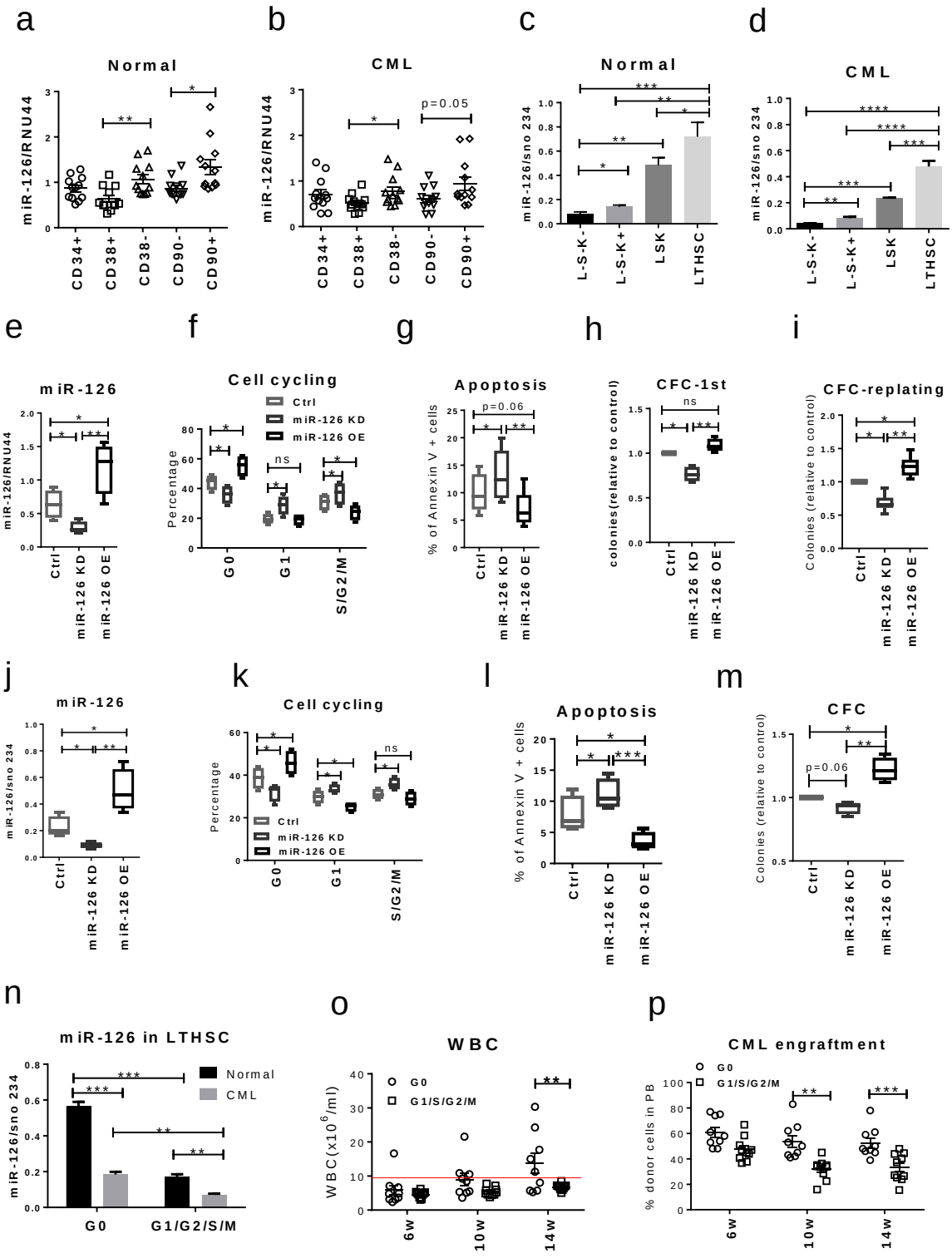

Figure 1: Human and mouse CML LSC express higher levels of miR-126

(a,b) QPCR for miR-126 expression in HPC [Lin^-CD34^+($CD34^+$) and $Lin^-CD34^+CD38^+$ ($CD38^+$)], HSC [$Lin^-CD34^+CD38^-$ ($CD38^-$) and $Lin^-CD34^+CD38^-CD90^-$ ($CD90^-$)] and LTHSC [$Lin^-CD34^+CD38^-CD90^+$ ($CD90^+$)] from (a) normal donors' (n=12) and (b) newly diagnosed CP CML patients' (n=12) blood and BM samples. (c-d) QPCR for miR-126 expression in BM subpopulations from normal and CML mice (n=6). CML $Lin^-CD34^+CD38^-$ cells were transduced with GFP-expressing miRZip anti-miR-126 (KD, MOI=20) or miR-126 precursor (OE, MOI=10) or control lentivirus (MOI=10-20). GFP^+ cells were selected and cultured for 72h and then (e) miR-126 expression, (f) cell cycling, (g) apoptosis, (h) CFC and (i) CFC replating efficiency were measured (n=4). LTHSC from induced SCLtTA/BCR-ABL mice were transduced with miR-126 KD, miR-126 OE, or control lentivirus (MOI=20). GFP^+ cells were cultured for 72h and (j) miR-126 expression, (k) cell cycling, (l) apoptosis, and (m) CFC were measured (n=4). Quiescent $Hoechst^-Pyronin^-$ (G0) LTHSC and proliferating $Hoechst^{+/-}Pyronin^+$ (G1/G2/S/M) LTHSC (CD45.2 B6) were sorted and transplanted into recipient mice (CD45.1 B6, n=10). (n) QPCR for miR-126 expression in quiescent and proliferating LTHSC (n=3). (o) White blood cell (WBC) counts and (p) donor CML cell engraftment in PB of the recipient mice were measured (n=10).

Figure 2

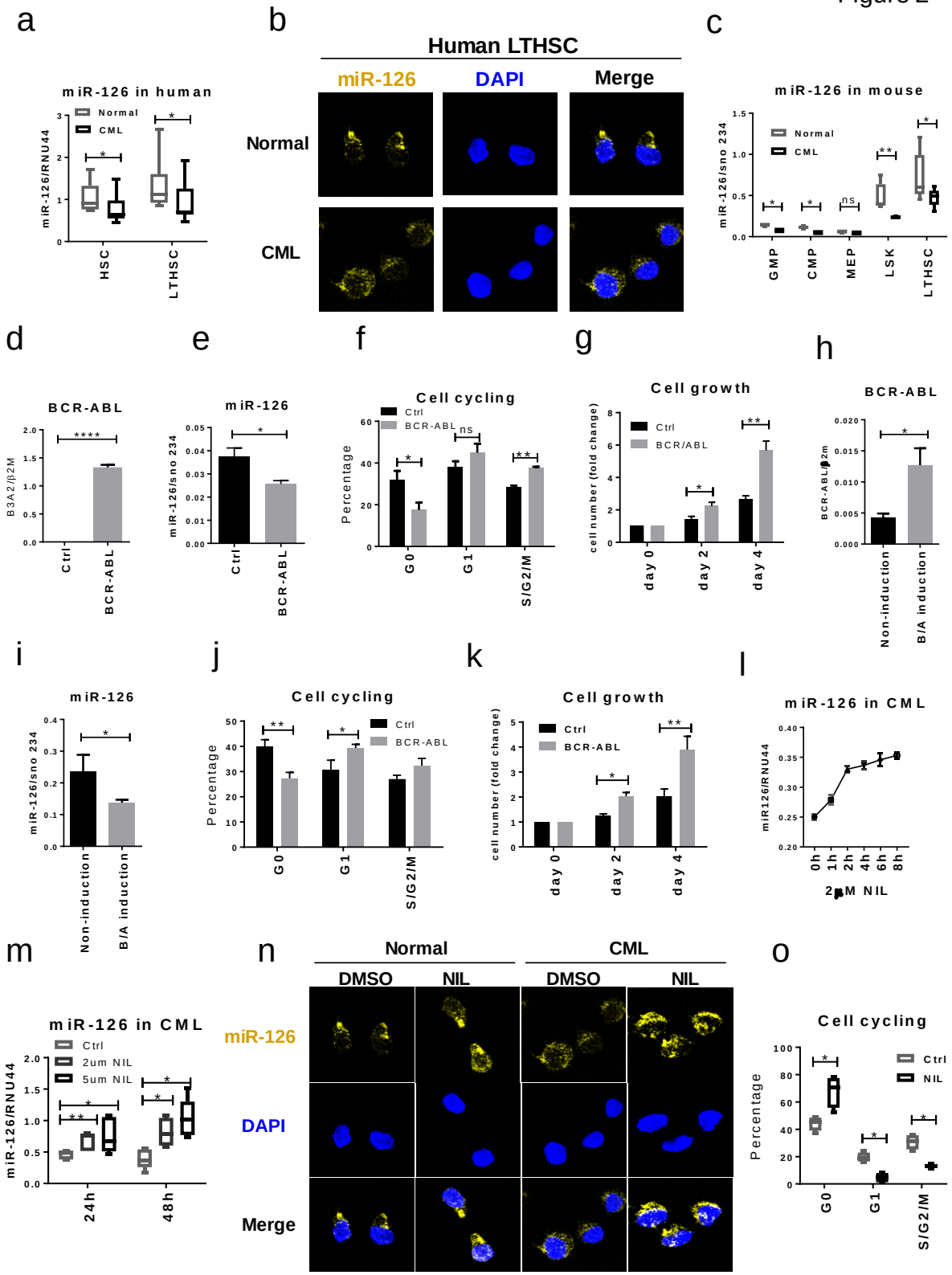
a
miR-126 in human
Normal
CML
miR-126/RNU44
HSC
LTHSC
b
Human LTHSC
miR-126
DAPI
Merge
Normal
CML
c
miR-126 in mouse
Normal
CML
miR-126/sno 234
GMP
CMP
MEP
LSK
LTHSC
d
BCR-ABL
B3A2/β2M
Ctrl
BCR-ABL
e
miR-126
miR-126/sno 234
Ctrl
BCR-ABL
f
Cell cycling
Ctrl
BCR-ABL
Percentage
G0
G1
S/G2/M
g
Cell growth
Ctrl
BCR/ABL
cell number (fold change)
day 0
day 2
day 4
h
BCR-ABL
BCR-ABL/β2m
Non-induction
B/A induction
i
miR-126
miR-126/sno 234
Non-induction
B/A induction
j
Cell cycling
Ctrl
BCR-ABL
Percentage
G0
G1
S/G2/M
k
Cell growth
Ctrl
BCR-ABL
cell number (fold change)
day 0
day 2
day 4
l
miR-126 in CML
miR126/RNU44
0h
1h
2h
4h
6h
8h
2μM NIL
m
miR-126 in CML
Ctrl
2um NIL
5um NIL
miR-126/RNU44
24h
48h
n
Normal
CML
DMSO
NIL
DMSO
NIL
miR-126
DAPI
Merge
o
Cell cycling
Ctrl
NIL
Percentage
G0
G1
S/G2/M

Figure 2: BCR-ABL down-regulates miR-126 expression in CML cells

(a-b) miR-126 expression in normal and CML cell populations from human samples (a) by QPCR (n=10) and (b) by miRNA staining and (c) from mouse BM by QPCR (n=6). Normal mouse BM LSK cells were sorted and transduced with a retroviral *BCR-ABL* or control construct. (d) *BCR-ABL* and (e) miR-126 expression (n=4) were measured by QPCR at 24h after transduction. (f) Cell cycling and (g) cell growth (n=3) at 48h after transduction are shown. LTHSC from non-induced BCR-ABL transgenic mice (tet off) were sorted and cultured in the presence or absence of tetracycline (2µg/ml) to induce BCR-ABL. (h) *BCR-ABL* expression and (i) miR-126 levels (n=3) were measured by QPCR. (j) Cell cycling and (k) cell growth (n=3) were measured at 48h after BCR-ABL induction. (l-n) miR-126 expression (n=3) in (l-m) human CML $Lin^-CD34^+CD38^-$ cells treated with and without NIL by QPCR and in (n) normal and CML $Lin^-CD34^+CD38^-$ cells treated with and without NIL by miRNA staining and (o) cell cycling (n=4) of human CML $Lin^-CD34^+CD38^-$ cells treated with and without NIL.

Figure 3

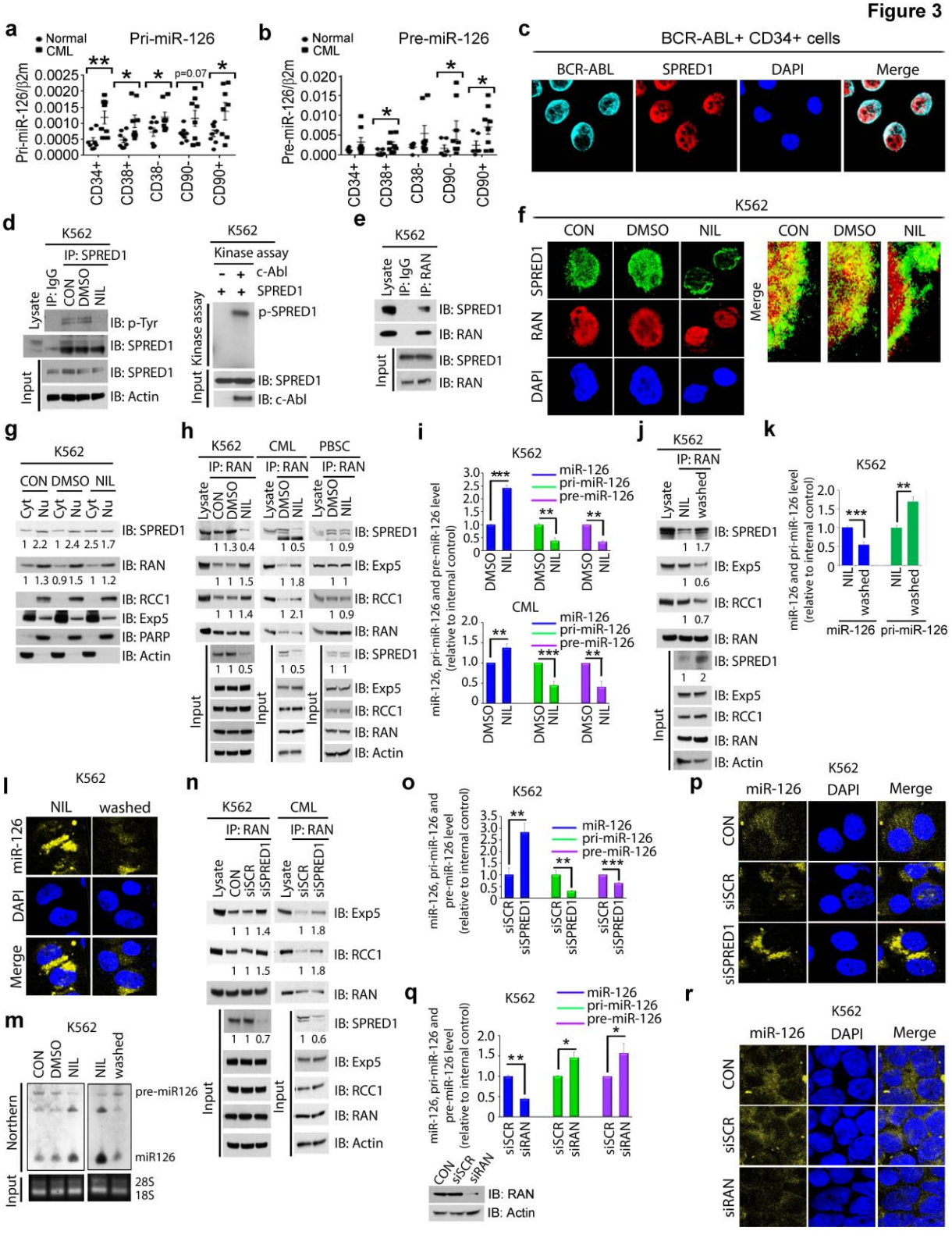
a
Normal
CML
Pri-miR-126
Pri-miR-126/β2m
CD34+
CD38+
CD38-
CD90-
CD90+
p=0.07
b
Pre-miR-126
Pre-miR-126/β2m
c
BCR-ABL+ CD34+ cells
BCR-ABL
SPRED1
DAPI
Merge
d
K562
IP: SPRED1
IP: IgG
CON
DMSO
NIL
Lysate
Input
IB: p-Tyr
IB: SPRED1
IB: Actin
Kinase assay
c-Abl
p-SPRED1
IB: c-Abl
e
IP: RAN
IB: RAN
f
CON
DMSO
NIL
SPRED1
RAN
DAPI
Merge
g
Cyt
Nu
IB: PARP
h
CML
PBSC
IP: RAN
i
miR-126
pri-miR-126
pre-miR-126
miR-126, pri-miR-126 and pre-miR-126 level (relative to internal control)
j
washed
k
miR-126 and pri-miR-126 level (relative to internal control)
l
miR-126
DAPI
Merge
m
Northern
pre-miR126
miR126
28S
18S
n
siSCR
siSPRED1
siRAN
o
p
q
r

Figure 3: **BCR-ABL deregulates miR-126 biogenesis**

(a) pri-miR-126 (n=8) and (b) pre-miR-126 expression levels by QPCR (n=8) in human normal and CML cell populations. (c) BCR-ABL and SPRED1 co-staining in CML $CD34^+$ cells by immunofluorescence (IF). K562 cells were treated with or without NIL for 24h and protein lysates were collected. (d) Immunoprecipitation (IP) with anti-SPRED1 and immunoblotting with anti-SPRED1 and anti-phosphotyrosine (p-Tyr) antibodies and *in vitro* kinase assay by IP with anti-c-Abl and immunoblotting with anti-SPRED1. (e) IP with anti-RAN and immunoblotting with anti-SPRED1 and anti-RAN antibodies were performed with K562 cells. (f) IF co-staining of SPRED1 and RAN in K562 cells treated with and without NIL. (g) SPRED1, RAN, RCC1 and Exp-5 expression in cytoplasmic (cyt) and nuclear (nu) fractions from K562 cells, treated with and without NIL, was measured by western blot. Densitometric quantification (normalized to internal control) is shown under the blots. (h) IP with anti-RAN and immunoblotting with anti-SPRED1, RAN, Exp-5 and RCC1 antibodies were performed with K562 cells as well as normal and CML $CD34^+$ cells treated with and without NIL. Densitometric quantification (normalized to internal control) is shown under the blots. (i) QPCR for mature, pri- and pre-miR-126 expression in K562 and CML $CD34^+$ cells treated with and without NIL (n=3). (j) IP with anti-RAN and immunoblotting with anti-SPRED1, Exp-5, RCC1 and RAN antibodies were performed with K562 cells with or without TKI washing-off. Densitometric quantification is shown under the blots. (k) QPCR for mature and pri-miR-126 expression (n=3), (l) miR-126 staining, and (m) mature and pre-miR-126 levels measured by Northern blotting in K562 cells. (n) SPRED1 was knocked down in K562 and CML $CD34^+$ cells and protein lysates were pulled down by anti-RAN and immunoblotted with anti-Exp-5, RCC1 and RAN antibodies. Densitometric quantification (normalized to internal control) is shown under the blots. (o) QPCR for mature, pri- and pre-miR-126 expression (n=3) and (p) miR-126 staining in SPRED1 KD K562 cells. (q) QPCR for mature, pri- and pre-miR-126 expression (n=3) and (r) miR-126 staining in RAN KD K562 cells.

Figure 4

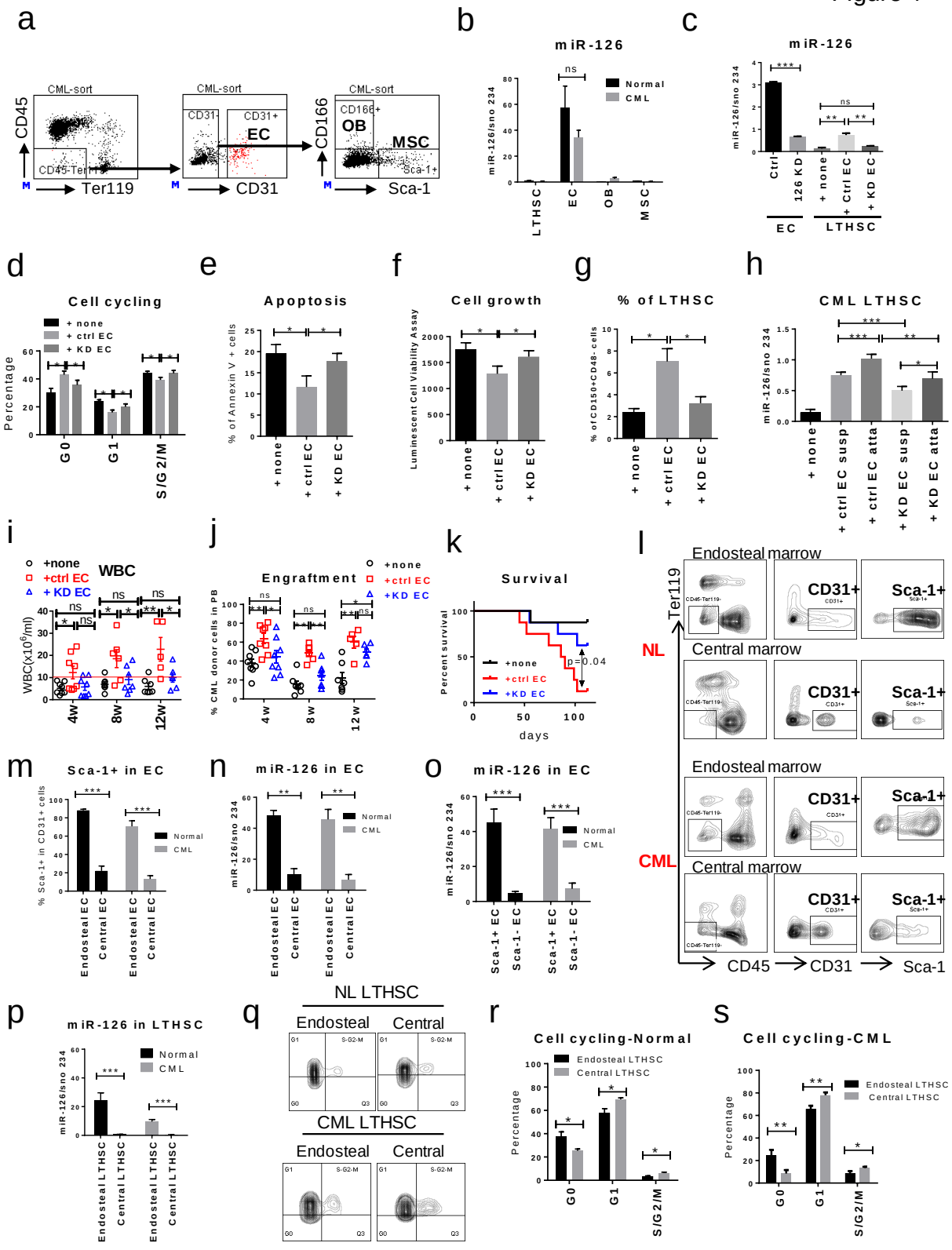
a
CML-sort
CD45
CD45-Ter119+
Ter119
CD31
CD31+
EC
Sca-1
CD166+
OB
MSC
Sca-1+
b
miR-126
miR-126/sno 234
Normal
CML
LTHSC
EC
OB
MSC
c
miR-126
Ctrl
126 KD
+ none
+ Ctrl EC
+ KD EC
EC
LTHSC
d
Cell cycling
Percentage
G0
G1
S/G2/M
e
Apoptosis
% of Annexin V + cells
f
Cell growth
Luminescent Cell Viability Assay
g
% of LTHSC
% of CD150+CD48- cells
h
CML LTHSC
+ ctrl EC susp
+ ctrl EC atta
+ KD EC susp
+ KD EC atta
i
WBC
+none
+ctrl EC
+KD EC
WBC(x10^6/ml)
4w
8w
12w
j
Engraftment
% CML donor cells in PB
k
Survival
Percent survival
p=0.04
days
l
Endosteal marrow
Central marrow
NL
CML
Ter119
CD31+
Sca-1+
CD45
CD31
Sca-1
m
Sca-1+ in EC
% Sca-1+ in CD31+ cells
Endosteal EC
Central EC
n
miR-126 in EC
o
miR-126 in EC
Sca-1+ EC
Sca-1- EC
p
miR-126 in LTHSC
Endosteal LTHSC
Central LTHSC
q
NL LTHSC
Endosteal
Central
CML LTHSC
r
Cell cycling-Normal
Endosteal LTHSC
Central LTHSC
s
Cell cycling-CML

Figure 4: Endothelial cells in the niche supply miR-126 to normal and CML LTHSC

(a) Gating strategy of EC ($CD45^-Ter119^-CD31^+$), osteoblasts (OB, $CD45^-Ter119^-CD31^-CD166^+Sca\text{-}1^-$) and mesenchymal stem cells (MSC, $CD45^-Ter119^-CD31^-CD166^-Sca\text{-}1^+$). (b) miR-126 expression by QPCR in LTHSC, EC, OB and MSC cells from normal and CML mice (n=5). EC were then sorted from the BM of SCLtTA/BCR-ABL mice and transduced with miR-126 KD lentiviral vector (KD EC) or control vector (ctrl EC). CML LTHSC were sorted and co-cultured with ctrl or KD EC or cultured alone (none) for 96h and (c) miR-126 expression (n=4), (d) cell cycling (n=3), (e) apoptosis (n=4), (f) cell growth (n=4) and (g) percentage of $Flt3^-CD150^+CD48^-$ LSK cells (n=4) were measured. (h) Suspended (susp) and EC-attached (atta) sub-fractions of CML LTHSC were collected and miR-126 expression was measured by QPCR (n=3). CML LTHSC (CD45.2 B6) were sorted and co-cultured with ctrl or KD EC or none for 96h and then transplanted into recipient mice (CD45.1 B6, 1000 cells/mouse, n=8 each). (i) WBC and (j) CML donor cell engraftment in PB and (k) survival of recipient mice were monitored. (l) Representative flow cytometry plots of EC staining and (m) frequency of $Sca\text{-}1^+$ cells in endosteal EC or central EC from normal and CML mice (n=3) and (n-o) miR-126 expression in endosteal EC or central EC (n=3) and in $Sca\text{-}1^{+/-}$ EC (n=3) from normal and CML mice by QPCR. (p) miR-126 expression by QPCR in endosteal LTHSC or central LTHSC from normal and CML mice (n=3). (q) Representative flow cytometry plots and (r-s) combined results of cell cycling (n=3) of endosteal LTHSC or central LTHSC from normal and CML mice.

Figure 5

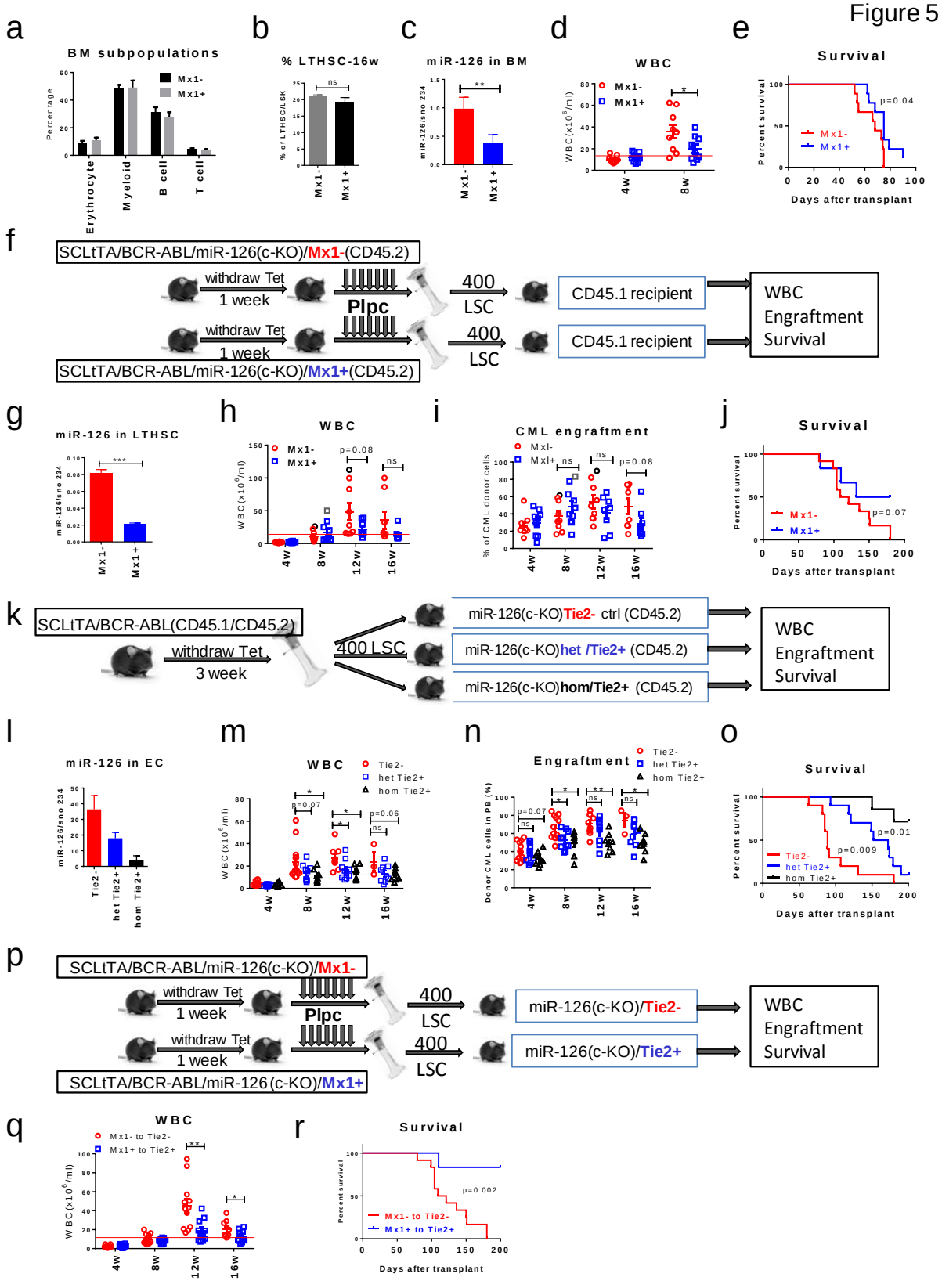
a
BM subpopulations
Mx1-
Mx1+
Percentage
Erythrocyte
Myeloid
B cell
T cell
b
% LTHSC-16w
ns
% of LTHSC/LSK
Mx1-
Mx1+
c
miR-126 in BM
**
miR-126/sno 234
Mx1-
Mx1+
d
WBC
Mx1-
Mx1+
*
WBC(x10^6/ml)
4w
8w
e
Survival
p=0.04
Mx1-
Mx1+
Percent survival
Days after transplant
f
SCLtTA/BCR-ABL/miR-126(c-KO)/Mx1-(CD45.2)
withdraw Tet
1 week
Plpc
400
LSC
CD45.1 recipient
withdraw Tet
1 week
400
LSC
CD45.1 recipient
SCLtTA/BCR-ABL/miR-126(c-KO)/Mx1+(CD45.2)
WBC
Engraftment
Survival
g
miR-126 in LTHSC
***
miR-126/sno 234
Mx1-
Mx1+
h
WBC
Mx1-
Mx1+
p=0.08
ns
WBC(x10^6/ml)
4w
8w
12w
16w
i
CML engraftment
Mxl-
Mxl+
ns
ns
p=0.08
% of CML donor cells
4w
8w
12w
16w
j
Survival
Mx1-
Mx1+
p=0.07
Percent survival
Days after transplant
k
SCLtTA/BCR-ABL(CD45.1/CD45.2)
withdraw Tet
3 week
400 LSC
miR-126(c-KO)Tie2- ctrl (CD45.2)
miR-126(c-KO)het /Tie2+ (CD45.2)
miR-126(c-KO)hom/Tie2+ (CD45.2)
WBC
Engraftment
Survival
l
miR-126 in EC
miR-126/sno 234
Tie2-
het Tie2+
hom Tie2+
m
WBC
Tie2-
het Tie2+
hom Tie2+
p=0.07
p=0.06
WBC(x10^6/ml)
4w
8w
12w
16w
n
Engraftment
Tie2-
het Tie2+
hom Tie2+
p=0.07
Donor CML cells in PB (%)
4w
8w
12w
16w
o
Survival
p=0.01
p=0.009
Tie2-
het Tie2+
hom Tie2+
Percent survival
Days after transplant
p
SCLtTA/BCR-ABL/miR-126(c-KO)/Mx1-
withdraw Tet
1 week
Plpc
400
LSC
miR-126(c-KO)/Tie2-
withdraw Tet
1 week
400
LSC
miR-126(c-KO)/Tie2+
SCLtTA/BCR-ABL/miR-126(c-KO)/Mx1+
WBC
Engraftment
Survival
q
WBC
Mx1- to Tie2-
Mx1+ to Tie2+
**
*
WBC(x10^6/ml)
4w
8w
12w
16w
r
Survival
p=0.002
Mx1- to Tie2-
Mx1+ to Tie2+
Percent survival
Days after transplant

Figure 5: Endothelial cells in the niche supply miR-126 to CML LTHSC

(a) Frequency of BM mononuclear cell subpopulations (n=5) and (b) LTHSC (n=5) in miR-126(c-KO)/Mx1-cre+ (Mx1+) and miR-126(c-KO)/Mx1-cre- (Mx1-) mice at 16 weeks after pIpC injection to induce “cre” activation and miR-126 KD. (c) miR-126 expression in CML BM cells (n=4), (d) WBC and (e) survival of SCLtTA/BCR-ABL/miR-126(c-KO)/Mx1+/- mice subjected to tetracycline withdrawal to induce BCR-ABL expression and pIpC injection to induce miR-126 KD (n=9). (f) CD45.2 CML LTHSC (400 cells/mouse) from BCR-ABL-induced and pIpC-injected SCLtTA/BCR-ABL/miR-126(c-KO)/Mx1+ or Mx1- mice were transplanted into CD45.1 congenic recipient mice by tail vein injection (n=10 for each group). (g) miR-126 expression in donor CML LTHSC by QPCR (n=3), (h) WBC and (i) CML cell engraftment in PB and (j) survival of recipient mice were monitored (n=10). In order to track donor cells in CD45.2 miR-126(c-KO)/Tie2+/- recipient mice, CD45.2 SCLtTA/BCR-ABL B6 mice were crossed with CD45.1 B6 mice to generate CD45.1/CD45.2 SCLtTA/BCR-ABL mice. (k) CD45.1/CD45.2 CML LTHSC (400 cells/mouse) from induced SCLtTA/BCR-ABL mice were transplanted into CD45.2 congenic miR-126(c-KO)/Tie2- (n=14), miR-126(c-KO)het/Tie2+ (n=10) and miR-126(c-KO)hom/Tie2+ recipient mice (n=8). (l) miR-126 expression in EC sorted from the miR-126(c-KO)/Tie2-, het/Tie2+ and hom/Tie2+ recipient mice by QPCR (n=3), (m) WBC and (n) CML cell engraftment in PB and (o) survival of recipient mice were monitored. (p) CD45.2 CML LTHSC (400 cells/mouse) from BCR-ABL-induced and pIpC-injected SCLtTA/BCR-ABL/miR-126(c-KO)/Mx1+ or Mx1- mice were transplanted into CD45.2 miR-126(c-KO)het/Tie2+ or Tie2- recipient mice (n=12 for each group), respectively and (q) WBC and (r) survival of the recipient mice was monitored.

Figure 6

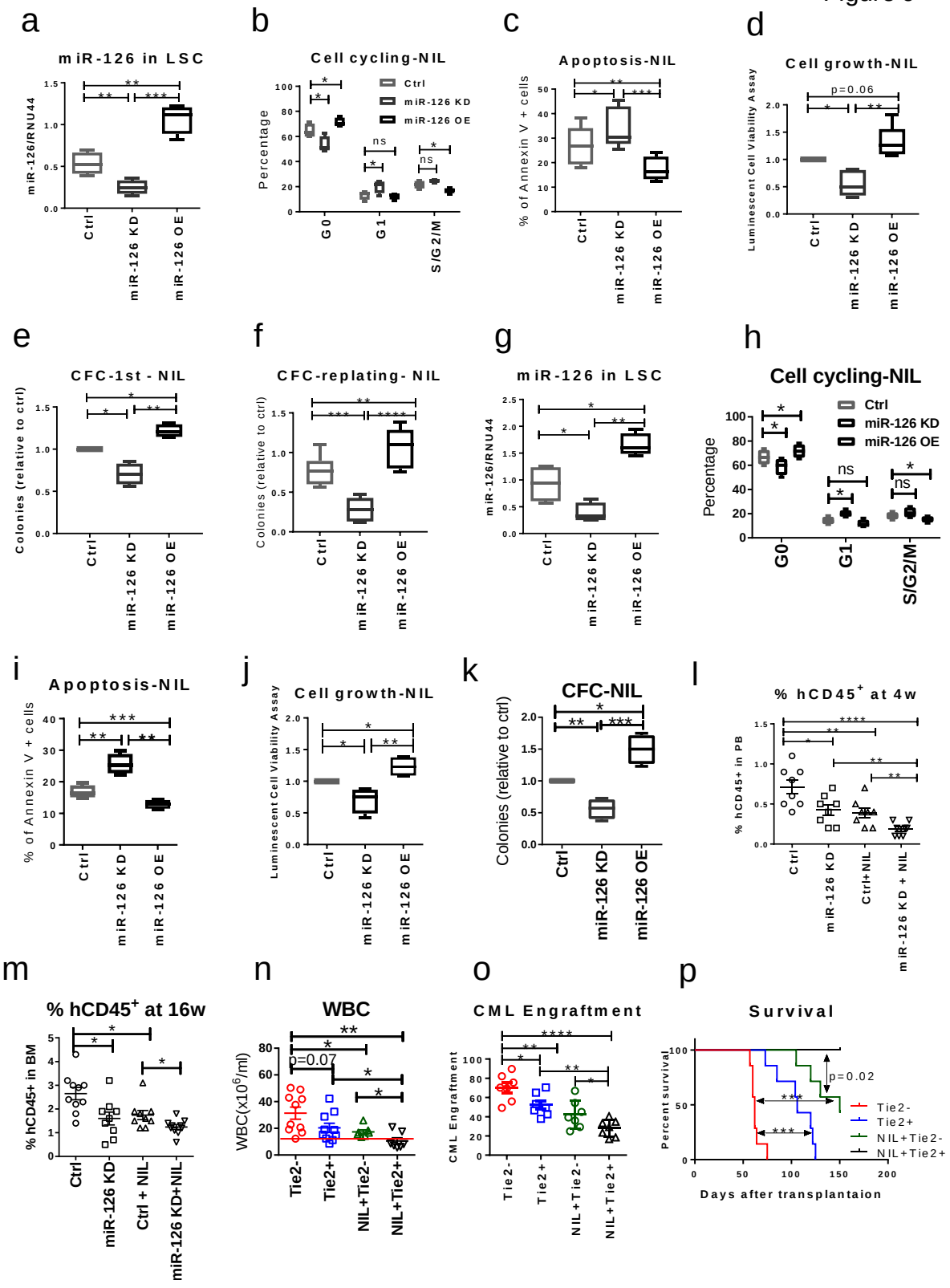
a
miR-126 in LSC
miR-126/RNU44
Ctrl
miR-126 KD
miR-126 OE
b
Cell cycling-NIL
Percentage
Ctrl
miR-126 KD
miR-126 OE
G0
G1
S/G2/M
ns
c
Apoptosis-NIL
% of Annexin V + cells
d
Cell growth-NIL
Luminescent Cell Viability Assay
p=0.06
e
CFC-1st - NIL
Colonies (relative to ctrl)
f
CFC-replating- NIL
g
miR-126 in LSC
h
Cell cycling-NIL
i
Apoptosis-NIL
j
Cell growth-NIL
k
CFC-NIL
l
% hCD45+ at 4w
% hCD45+ in PB
Ctrl+NIL
miR-126 KD + NIL
m
% hCD45+ at 16w
% hCD45+ in BM
Ctrl + NIL
miR-126 KD+NIL
n
WBC
WBC(x10^6/ml)
p=0.07
Tie2-
Tie2+
NIL+Tie2-
NIL+Tie2+
o
CML Engraftment
p
Survival
Percent survival
p=0.02
Days after transplantaion

Figure 6: miR-126 knockdown enhanced TKI-mediated targeting of CML LSC

CML $Lin^-CD34^+CD38^-$ cells were transduced with GFP-expressing miRZip anti-miR-126 (KD, MOI=20) or miR-126 precursor (OE, MOI=10) or control lentivirus (MOI=10-20). GFP^+ cells were selected and treated with NIL (5μM) for 72h and then (a) miR-126 expression, (b) cell cycling, (c) apoptosis, (d) cell growth, (e) CFC and (f) CFC replating efficiency were measured (n=4). LTHSC from induced SCLtTA/BCR-ABL mice were transduced with miR-126 KD or miR-126 OE or control lentivirus (MOI=20). GFP^+ cells were treated with NIL (5μM) for 72h and (g) miR-126 expression, (h) cell cycling, (i) apoptosis, (j) cell growth and (k) CFC were measured (n=4). Human CML $Lin^-CD34^+CD38^-$ cells were transduced with miR-126 KD or control lentiviral vector. GFP^+ cells were selected ($5X10^5$ cells/mouse, n=10 each) and treated with NIL (5μM) for 4 days and then transplanted into irradiated (300cGy) NSG-SGM3 mice. (l-m) Engraftment of human $CD45^+GFP^+$ cells in PB at 4 weeks (n=8) and in BM at 16 weeks (n=10) was measured. CML LTHSC from CD45.1/CD45.2 SCLtTA/BCR-ABL mice were transplanted into CD45.2 miR-126(c-KO)het/Tie2+ or Tie2- mice (n=17 each). Upon confirming development of CML, the mice were treated with (n=7 each) or without NIL (n=10 each) for 3 weeks, (n) WBC and (o) CML donor cell engraftment and (p) survival were monitored.

Figure 7

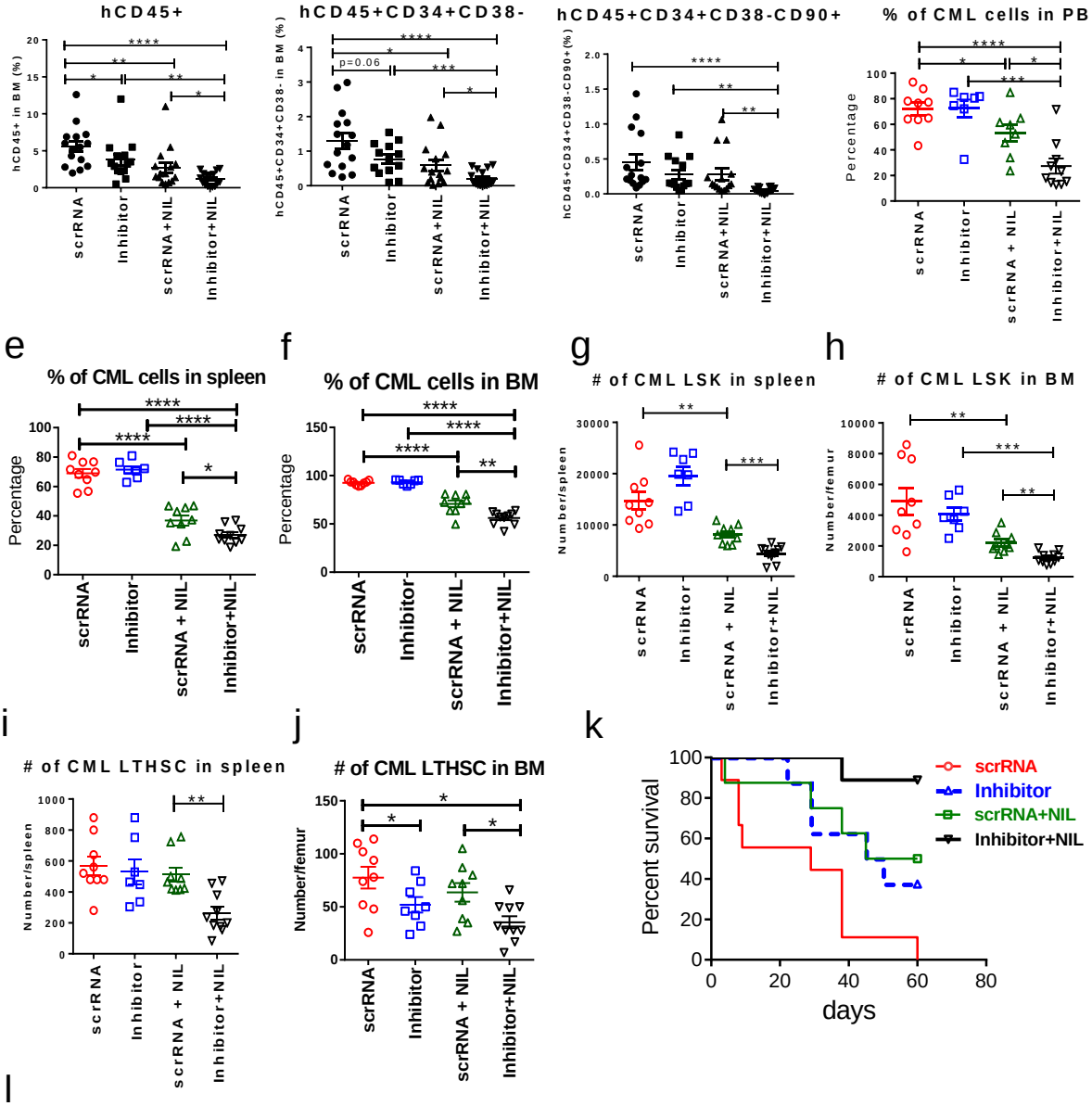

l

Cell dose/mouse	Leukemia developed/tested			
	scrRNA	Inhibitor	scrRNA+NIL	Inhibitor +NIL
4 million	6/6	2/6	3/6	0/6
2 million	2/6	1/6	3/6	0/6
1 million	2/6	0/6	2/6	0/6
0.5 million	1/6	0/6	0/6	0/6
Frequency of LIC	4.20E-07	7.54E-08	2.36E-07	0

Figure 7: CpG-miR-126 inhibitor enhances *in vivo* targeting of CML LSC in combination with Nilotinib

Human $CD34^+$ cells from CP CML patient samples were transplanted into irradiated NSG-SGM3 mice (n=56). At 6 weeks after transplantation, the mice were randomly divided into 4 groups (n=14 each) and treated with scrRNA (5mg/kg, i.v. 4 times a week), inhibitor (5mg/kg i.v. 4 times a week), scrRNA + NIL (50mg/kg, daily by gavage), or inhibitor + NIL for 3 weeks. (a) Human $CD45^+$, (b) $CD45^+CD34^+CD38^-$ HSC and (c) $CD45^+CD34^+CD38^-CD90^+$ LTHSC engraftment in BM was measured. CD45.2 BM cells from induced SCLtTA/BCR-ABL mice were transplanted into congenic CD45.1 B6 mice (n=40) to generate a cohort of mice with CML-like disease. Following confirmation of CML development at 4 weeks after transplantation, mice were randomly divided into 4 groups (n=10 each) and treated as above with scrRNA, inhibitor, scrRNA + NIL, or inhibitor + NIL for 3 weeks. Percentage of donor CML cells in (d) PB, (e) spleen and (f) BM, numbers of donor CML LSK in (g) spleen and (h) BM, and numbers of donor CML LTHSC in (i) spleen and (j) BM after 3 weeks' treatment were measured. (k) Another cohort of mice was treated for 3 weeks and then followed for survival (n=10 in each group). BM cells (CD45.2) from treated leukemic mice (3 weeks) were pooled, and 4×10^6, 2×10^6, 1×10^6, and 5×10^5 cells/mouse were transplanted into secondary congenic CD45.1 recipient mice (n=6 mice/dose/condition x 4 doses x 4 conditions = 96 mice). The recipient mice were monitored for 16 weeks for CML cell engraftment in blood and leukemia development by WBC counts. (l) Frequency of leukemia initiating cells (LIC) was quantified using L-Calc software.